RNA (2002), *8*:798–815. Cambridge University Press. Printed in the USA.

DOI: 10.1017.S1355838202025050

Characterization of interactions among the Cef1p-Prp19p-associated splicing complex

MELANIE D. OHI and KATHLEEN L. GOULD

Howard Hughes Medical Institute and Department of Cell Biology, Vanderbilt University School of Medicine, Nashville, Tennessee 37232, USA

ABSTRACT

***Schizosaccharomyces pombe* (*Sp*) Cdc5p and its *Saccharomyces cerevisiae* (*Sc*) ortholog, Cef1p, are essential components of the spliceosome. In *S. cerevisiae,* a subcomplex of the spliceosome that includes Cef1p can be isolated on its own; this has been termed the nineteen complex (Ntc) because it contains Prp19p. Components of the Ntc include Cef1p, Snt309p, Syf2p/Ntc31p, Ntc30p/Isy1p, Ntc20p and at least six unidentified proteins. We recently identified ~30 proteins that copurified with Cdc5p and Cef1p. Previously unidentified *S. pombe* proteins in this purification were called Cwfs for complexed with five and novel *S. cerevisiae* proteins were called Cwcs for complexed with Cef1p. Using these proteomics data coupled with available information regarding Ntc composition, we have investigated protein identities and interactions among Ntc components. Our data indicate that Cwc2p, Prp46p, Clf1p, and Syf1p most likely represent Ntc40p, Ntc50p, Ntc77p, and Ntc90p, respectively. We show that *Sc* Cwc2p interacts with Prp19p and is involved in pre-mRNA splicing. *Sp cwf2*$^{+}$, the homolog of *Sc CWC2*, is allelic with the previously identified *Sp prp3*$^{+}$. We present evidence that *Sp* Cwf7p, an essential protein with obvious homologs in many eukaryotes but not *S. cerevisiae*, is a functional counterpart of *Sc* Snt309p and binds *Sp* Cwf8p (a homolog of *Sc* Prp19p). Further, our data indicate that a mutation in the U-box of Prp19p disrupts these numerous protein interactions causing Cef1p degradation and Ntc instability.**

Keywords: Cdc5p; Cef1p; Cwc complex; Cwc2p; Cwf complex; Cwf2p; Cwf7p; Myb; Ntc complex; Ntc40p; pre-mRNA splicing; Prp19p; Prp46p; Snt309p

INTRODUCTION

The spliceosome is a dynamic multiprotein/RNA complex that catalyzes the excision of introns from pre-mRNA. Five snRNA molecules (U1, U2, U4, U5, and U6) that are closely associated with conserved protein components play key roles in the pre-mRNA processing reaction. These snRNA/protein combinations are referred to as small nuclear ribonucleoprotein particles (snRNPs). A popular model for snRNP assembly into an active spliceosome was developed from in vitro splicing experiments (reviewed in Kramer, 1996; Staley & Guthrie, 1998; Murray & Jarrell, 1999). In this model, spliceosome assembly begins with the recognition of the 5′ and 3′ splice sites by the U1 snRNP and the U2 snRNP, respectively. The subsequent engagement of the U4/U6/U5 tri-snRNP triggers the unwinding of the U4/U6 snRNA duplex, which is replaced by a U2/U6 snRNA duplex. Furthermore the U1 snRNA base pairing at the 5′ splice site is disrupted and exchanged for base pairing between 5′ splice site and the U6 snRNA. The subsequent release of the U1 and U4 snRNPs marks the transition from the inactive to active spliceosome that, in this model, would contain only the U2, U5, and U6 snRNPs. However, recent work has challenged this model, suggesting that the spliceosome is preassembled in vivo in a complex that contains numerous proteins and all five snRNAs (Das et al., 2000; Maroney et al., 2000; Stevens et al., 2002). In addition to proteins that copurify with the five snRNAs, many other proteins are essential participants in the splicing reaction. To further understand pre-mRNA processing, it will be important to characterize the many protein–protein interactions found between pre-mRNA splicing factors.

The *cdc5*$^{+}$ gene was first identified in *Schizosaccharomyces pombe* based on the isolation of a temperature-sensitive mutant that arrested in the G2 phase of the cell

Reprint requests to: Kathleen L. Gould, Department of Cell Biology, Vanderbilt University School of Medicine, B2309 MCN, Nashville, Tennessee 37232, USA; e-mail: kathy.gould@mcmail.vanderbilt.edu.

cycle (*cdc5-120*). Cdc5p orthologs were subsequently identified and characterized in *Saccharomyces cerevisiae* (called Cef1p; Ohi et al., 1998), *Arabidopsis thaliana* (Hirayama & Shinozaki, 1996), *Drosophila melanogaster* (Ohi et al., 1998), *Caenorhabditis elegans* (Ohi et al., 1998), *Xenopus laevis* (Stukenberg et al., 1997), and *Homo sapiens* (hCDC5, Bernstein & Coughlin, 1997; Groenen et al., 1998; Ohi et al., 1998). Substantial evidence indicates that these proteins play an essential function in pre-mRNA splicing (Burns et al., 1999; Tsai et al., 1999; Ajuh et al., 2000) rather than cell cycle control. Genetic depletion of *Sp* Cdc5p or *Sc* Cef1p causes accumulation of unspliced mRNAs in vivo (Burns & Gould, 1999; McDonald et al., 1999; Tsai et al., 1999). Inactivation of Cef1p by antibody interference or immunodepletion of hCDC5 inhibits splicing in vitro (Tsai et al., 1999; Ajuh et al., 2000). Also, in *S. pombe*, *S. cerevisiae*, and human cells, Cdc5p, Cef1p, and hCDC5, respectively, are detected in spliceosomal complexes (Neubauer et al., 1998; McDonald et al., 1999; Tsai et al., 1999; Ajuh et al., 2000; Ohi et al., 2002).

In *S. cerevisiae*, Cef1p was found to copurify with and bind directly to the pre-mRNA splicing factor Prp19p (Tsai et al., 1999). Proteins copurifying with Prp19p have been termed the nineteen complex (Ntc). Members of this complex include Snt309p (Ntc25p), Syf2p (Ntc31p), Isy1p (Ntc30p), Ntc20p, and approximately six other polypeptides that were not identified (Ntc120p, Ntc90p, Ntc81p, Ntc77p, Ntc50p, and Ntc40p; Tarn et al., 1994; Chen et al., 1998, 2001, 2002; Tsai et al., 1999). Prp19p, Cef1p, and other identified Ntc components have been found to associate with snRNPs during the pre-mRNA splicing reaction (Tarn et al., 1993b, 1994; Chen et al., 1998, 2001, 2002; Burns et al., 1999; Tsai et al., 1999). Therefore it appears that the Ntc might represent a subcomplex of the spliceosome.

Because we are interested in the particular role Cdc5p/Cef1p plays in pre-mRNA processing, we have begun to investigate the full range of proteins with which it interacts. Using tandem affinity purification (TAP) followed by direct analysis of large protein complex (DALPC) tandem mass spectrometry (Link et al., 1999), we recently identified many proteins that stably associated with *Sp* Cdc5p (termed Cwfs for complexed with Cdc5p) and *Sc* Cef1p (termed Cwcs for complexed with Cef1p; Rigaut et al., 1999; Tasto et al., 2001; Ohi et al., 2002). This analysis indicated that the *Sp* Cdc5p- and the *Sc* Cef1p-containing complexes are nearly identical in composition and contain many known pre-mRNA splicing factors, the U2, U5, and U6 snRNAs, as well as previously uncharacterized proteins. A subset of these proteins were also identified as interacting with Prp19p as part of the systematic analysis of yeast protein complexes (Gavin et al., 2002).

In another approach described here, we performed a stringent two-hybrid screen, identified Prp19p as a Cef1p binding partner, and defined the regions of both proteins involved in their association. Starting with this interaction, we have extended the range of proteins binding to either Cef1p or Prp19p (*Sp* Cdc5p and Cwf8p) making use of data collected in our proteomics analyses of Cdc5p/Cef1p-associated proteins (McDonald et al., 1999; Ohi et al., 2002) and previous analysis of the Ntc complex (Tarn et al., 1994; Chen et al., 1998, 1999, 2001; Tsai et al., 1999). We discover that Snt309p has functional homologs in other eukaryotes and assign identities to unknown Ntc components. We have also studied the consequence of a mutation within the U-box of Prp19p to the integrity of the complex. These data set the foundation for understanding the molecular architecture of this essential protein unit within the spliceosome.

RESULTS

Cef1p and Prp19p interact through conserved regions of each protein

To identify protein–protein interactions that tether Cef1p to the other components of the Ntc complex, we performed two-hybrid screens looking for Cef1p-interacting proteins. Given that we could expect multiple interactions between Cef1p and associated proteins (Chen et al., 1998, 1999; McDonald et al., 1999; Tsai et al., 1999; Ben-Yehuda et al., 2000a; Ohi et al., 2002) that would not necessarily reflect direct protein binding, we chose a two-hybrid system that scores only high affinity interactions (James et al., 1996). Using this approach, *PRP19* (Cheng et al., 1993) was the only clone isolated that interacted with *CEF1*. Prp19p is a splicing factor (Tarn et al., 1993a) that was previously found to interact directly with Cef1p by far western analysis (Tsai et al., 1999). We identified the *S. pombe* homolog of Prp19p, termed Cwf8p, in both our immuno affinity purification and TAP complex analysis of Cdc5p (McDonald et al., 1999; Ohi et al., 2002). Further, the mammalian PRP19 homolog (Q9UMS4) copurified with hCDC5 (Ajuh et al., 2000) suggesting that the interaction between these two proteins is highly conserved.

The region of Cef1p important for its interaction with Prp19p was deduced previously by deletion analysis in a two-hybrid assay. Removing a C-terminal portion of Cef1p eliminated its interaction with Prp19p, implying that this section may bind Prp19p (Tsai et al., 1999). To prove that this was the case and to fully define the Prp19p-binding region in Cef1p, we tested a series of *CEF1* constructs for their ability to support interaction with full-length *PRP19* in the two-hybrid system (Fig. 1A,B). As observed before (Tsai et al., 1999), full-length Cef1p and the C-terminus of Cef1p (CEF1.A) were able to interact with full-length Prp19p. As predicted by the deletion analysis, C-terminal fragments of Cef1p including residues 443–515 supported the Prp19p interaction (Fig. 1A,B).

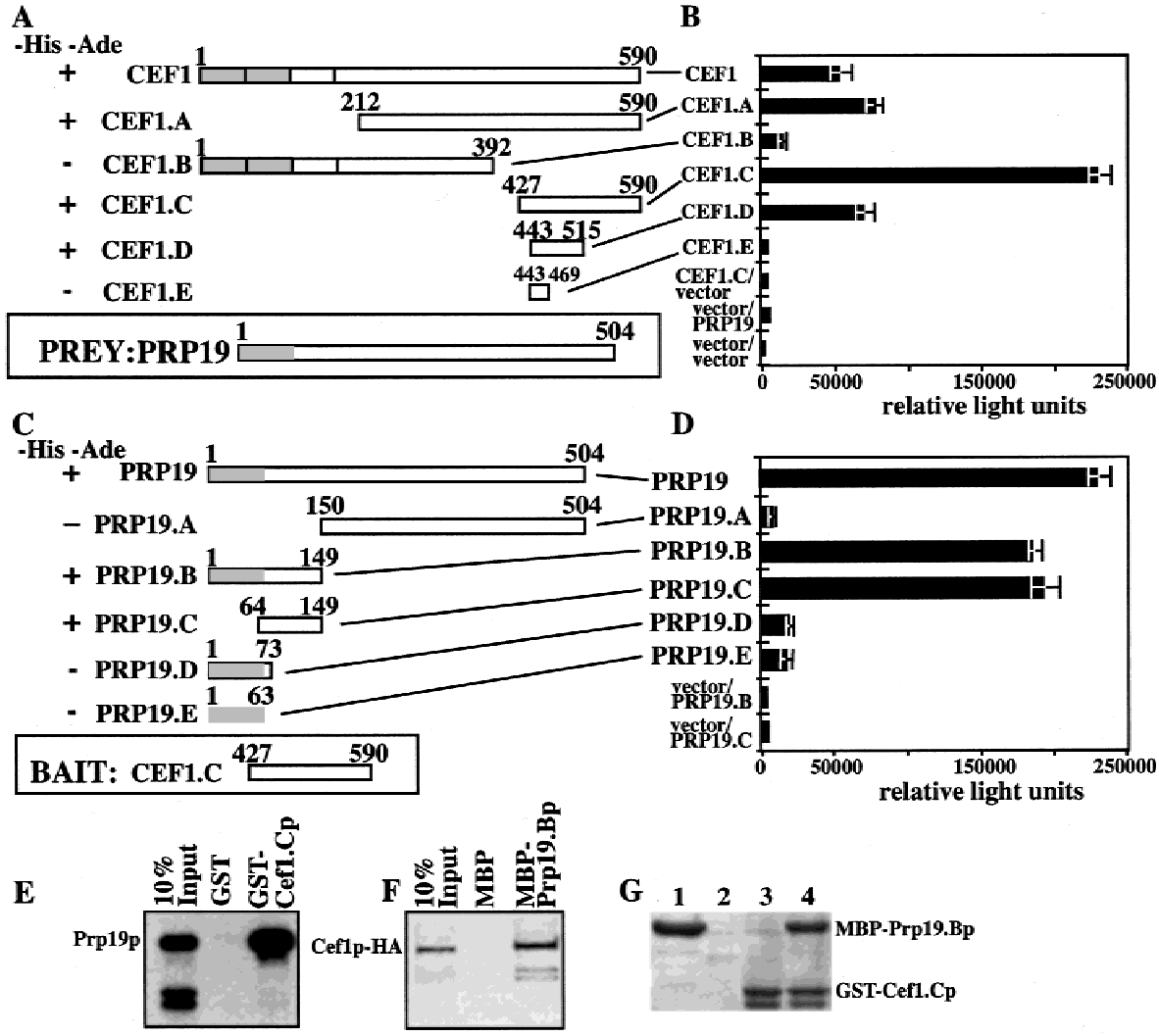

FIGURE 1. Definition of sequences supporting Cef1p–Prp19p interaction. **A:** PJ69-A was transformed with pGAD424PRP19 and pGBT9 carrying CEF1, CEF1.A, CEF1.B, CEF1.C, CEF1.D, or CEF1.E, which are shown schematically. Light shaded portions represent the Myb repeats, and the adjacent box depicts MLR3 (Ohi et al., 1998). + denotes growth and − represents no growth on selective media. **B:** β-galactosidase activity (represented by relative light units) of the strains described in **A**. **C:** The PJ69-4A strain was transformed with pGBT9CEF1 427–590 (CEF1.C) and pGAD424 carrying PRP19, PRP19.A, PRP19.B, PRP19.C, PRP19.D, or PRP19.E, which are shown schematically. The shaded portion represents the U-box motif. + denotes growth and − denotes no grow on selective media. **D:** β-galactosidase activity (represented by relative light units) of the strains described in **C**. **E:** GST or GST-Cef1p 427–590 bound to glutathione beads were mixed with in vitro-translated Prp19p. After extensive washes, the proteins were resolved by SDS-PAGE and autoradiography. "Input" represents a sample (1/10) of in vitro-translated Prp19p before the binding reaction. **F:** MBP or MBP-Prp19 1-149 (PRP19.B) bound to amylose were mixed with in vitro-translated Cef1p-HA. After extensive washes, the proteins were resolved by SDS-PAGE and autoradiography. "Input" represents a sample (1/10) of in vitro-translated Cef1p-HAp before the binding reaction. **G:** MBP-Prp19p 1-149 (PRP19.B) bound to amylose beads was mixed with soluble GST (lane 1). GST (lane 2) or GST-Cef1p 427–590 (CEF1.C) (lane 4) bound to glutathione beads were mixed with soluble MBP-Prp19p 1-149. GST-Cef1p 427–590 (CEF1.C) bound to glutathione beads was mixed with soluble MBP (lane 3). All binding reactions were washed extensively with binding buffer and proteins bound to the glutathione beads or amylose beads were eluted with sample buffer. Proteins in lanes 1–4 were visualized by Coomassie blue staining.

An alignment of Prp19p homologs illustrates a number of conserved domains that could be involved in mediating an interaction with CDC5 family members (Fig. 2). The PRP19 family of proteins share significant sequence identity throughout their entire lengths and contain two previously described protein motifs (Fig. 2). At the N-terminus, there is a 63-amino-acid stretch recently defined as a U-box. This motif is found in *Sc* Ufd2p and has been predicted to adopt a RING-like fold based on sequence-profile analysis (Aravind & Koonin, 2000). In addition to the U-box, Prp19p family members contain four WD40 repeats, motifs that are predicted to support specific protein–protein interactions (Smith et al., 1999).

To determine if these conserved domains in Prp19p are required for Cef1p interaction, we tested regions of

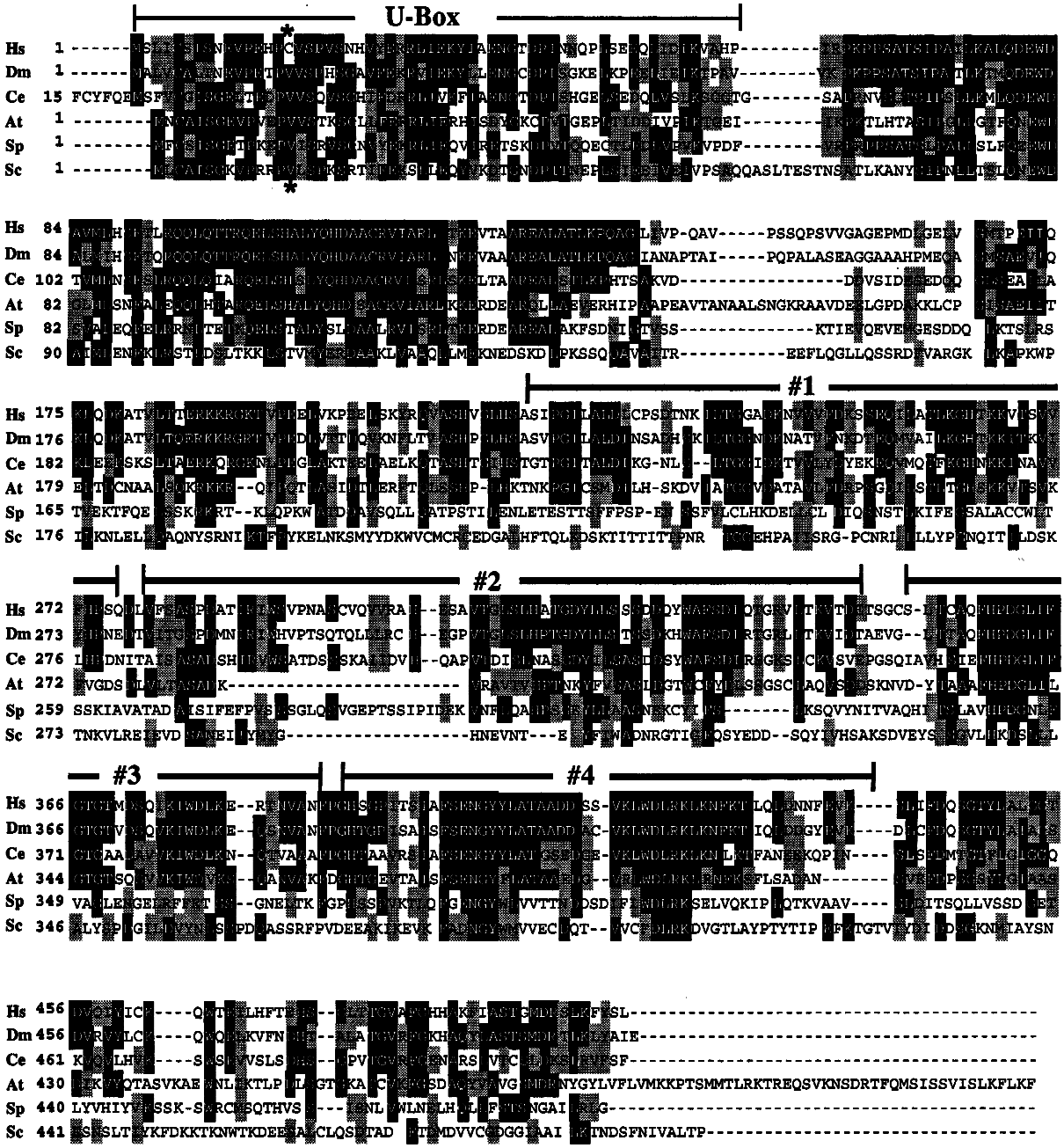

FIGURE 2. Alignment of PRP19 homologs. The ClustalW1.6 program (Thompson et al., 1994; Feng & Doolittle, 1996) was used to align Prp19p-related proteins from human (Hs; Q9UMS4), *D. melanogaster* (Dm; Q9V3B2), *C. elegans* (Ce; Q10051), *A. thaliana* (At; O22785), *S. pombe* (Sp; O14011), and *S. cerevisiae* (Sc; P32523). Residues found to be identical or similar to those of human PRP19 are highlighted in black or gray, respectively. The asterisk indicates the position of the mutation encoded by the *Sc prp19-1* allele. The U-box (Aravind & Koonin, 2000), a conserved 63-amino-acid motif, is labeled. Numbers bracketed by bars indicate the position of four WD40 repeats (Smith et al., 1999).

Prp19p for their ability to interact with Cef1p 427–590 (CEF1.C) in the two-hybrid system (Fig. 1C,D). The N-terminal segments of Prp19p interacted with Cef1p, whereas the C-terminal segments of Prp19p did not (Fig. 1C,D). Interestingly, the U-box domain (residues 1–63; PRP19.E) is dispensable for the Cef1p–Prp19p interaction (Fig. 1C,D). We conclude that residues 64–149 of Prp19p are sufficient to support an interaction with Cef1p. Although lacking a recognizable protein motif, residues 64–149 encompass a conserved sequence element (Fig. 2).

To show that the binding regions mapped in Prp19p and Cef1p are sufficient for supporting direct interaction between these proteins, in vitro binding assays were performed. GST-Cef1p 427–590, but not GST alone, bound labeled in vitro-translated Prp19p (Fig. 1E).

In a reciprocal experiment, MBP-Prp19p 1–149, but not MBP alone, bound labeled in vitro-translated Cef1p-HA (Fig. 1F). Furthermore, GST-Cef1p 427–590, but not GST alone, bound to MBP-Prp19p 1–149 (Fig. 1G, lanes 1–4).

Snt309p interacts with Prp19p but not with Cef1p

Although Cef1p and Prp19p interact directly in vitro (Fig. 1; Tsai et al., 1999), this interaction requires Snt309p at elevated temperatures in vivo (Chen et al., 1999). Snt309p is a nonessential protein identified in a synthetic lethal screen with *prp19-4* and is required for in vitro splicing at elevated temperatures (Chen et al., 1998). Further, Snt309p interacts with Prp19p, but not with Cef1p, by far western analysis (Chen et al., 1998). To help explain the role of Snt309p in maintaining Cef1p–Prp19p interaction in vivo, the region of Prp19p required for its interaction with Snt309p was mapped using the two-hybrid assay. As expected, full-length Prp19p was capable of interacting with Snt309p (Fig. 3A,B). Neither the C-terminus of Prp19p, spanning amino acids 150–504 (Prp19.A) nor the Prp19p U-box domain (PRP19.E) are required for this interaction. However both Prp19p 64–149 (PRP19.C) and Prp19p 1–73 (PRP19.D) interacted with Snt309p (Fig. 3A,B), indicating that the residues between 64 and 73 are critical for this association. Because Cef1p does not interact with Prp19p 1–73 (PRP19.D) but does interact with Prp19p 64–149 (Fig. 1C,D), the binding sites for Snt309p and Cef1p on Prp19p are not identical. These results are consistent with the interpretation that Cef1p and Snt309p associate independently with Prp19p. However, the proximity of the binding sites suggests that Snt309p binding might influence the local structure of Prp19p with consequence to Cef1p binding in vivo. The proximity of the two binding sites also raised the possibility that Snt309p might interact with Cef1p. However, we obtained no evidence for a direct Cef1p–Snt309p interaction in either the two-hybrid or the reticulocyte lysate systems (Fig. 3A,B; data not shown), results consistent with the inability of Snt309p to bind Cef1p by far western analysis (Chen et al., 1998).

Genetic interactions among *CEF1*, *SNT309*, and *PRP19*

The importance of these protein–protein interactions in vivo was confirmed by genetic analyses. First, we tested whether overexpression of the various genes could suppress temperature-sensitive phenotypes of *cef1-13* (Burns et al., 2002), *prp19-1* (Chen et al., 1998), or *snt309*Δ (Chen et al., 1998) strains. Overexpression of *CEF1* or *SNT309* but not *PRP19* or *PRP19.B* rescued growth of *cef1-13* at 36 °C (Fig. 4A). *prp19-1* cells overexpressing *PRP19* or *PRP19.B* grew at the restrictive temperature, whereas the overexpression of *CEF1* or *SNT309* did not rescue *prp19-1* growth (Fig. 4A). *SNT309*Δ cells were rescued at 36 °C by the overexpression of *SNT309* and *PRP19*, but not by the overexpression of *CEF1* or *PRP19.B* (Fig. 4A).

Second, we examined whether there were synthetic lethal interactions between *cef1-13*, *prp19-1,* and *snt309*Δ*.* The *cef1-1 prp19-1* and the *cef1-13 snt309*Δ double mutants were able to form colonies on medium selecting for a *CEF1*-expressing plasmid, but they were inviable on medium containing 5-FOA (Fig. 4B,C). We conclude that *cef1-13* is synthetically lethal with both *prp19-1* and *snt309*Δ.

SNT309 was isolated in a synthetic lethal screen with *prp19-4* (Chen et al., 1998). Surprisingly these authors did not find that *snt309*Δ and *prp19-1* were synthetically lethal. The ability of increased *PRP19* expression to suppress *snt309*Δ led us to reexamine this genetic interaction. A CEN *URA3*-marked plasmid carrying a genomic clone of *PRP19* was introduced into a *MATa/α prp19-1/PRP19 snt309*Δ*/SNT309* double heterozygote prior to sporulation. A haploid double mutant strain carrying the plasmid was isolated. Although the *prp19-1 snt309*Δ double mutant was able to form colonies on medium selecting for the *PRP19*-expressing plasmid, it was inviable on medium containing 5-FOA (Fig. 4D). Thus, we conclude that *prp19-1* and *snt309*Δ are synthetically lethal. In sum, these numerous genetic interactions support the importance of the direct physical associations described above.

Sp Cwf7p is a functional counterpart of *Sc* Snt309p

Sp Cwf7p was identified in all of our *Sp* Cdc5p purifications. Cwf7p is an essential splicing factor (Ohi et al., 2002) that has obvious homologs in other organisms (*D. melanogaster* Q9VAY6 and *C. elegans* Q22417). Its human homolog, SPF27 (*Human* O75934) copurified with hCDC5 in a core of four proteins, suggesting that it closely associates with hCDC5 (Ajuh et al., 2000). Although no similar protein was detected in the *S. cerevisiae* database, *Sc* Snt309p is of similar molecular weight and associates with Prp19p. For these reasons, we asked whether *Sp* Cwf7p might be a functional homolog of *Sc* Snt309p. We first tested whether *Sp* Cwf7p interacted with *Sp* Cwf8p (Cwf8p is the *S. pombe* homolog of Prp19p) in the two-hybrid system. A fragment encompassing the entire C-terminus of Cwf8p (cwf8.A) or just amino acids 57–141 (cwf8.B) supported a two-hybrid interaction with Cwf7p (Fig. 3C,D). Therefore, homologous sequence elements mediate Snt309p-Prp19p and Cwf7p-Cwf8p interactions. Further, overexpression of the *cwf7*$^{+}$cDNA rescued growth of *snt309*Δ cells at 36 °C (Fig. 3E). We conclude that *Sp* Cwf7p is a functional homolog of *Sc* Snt309p.

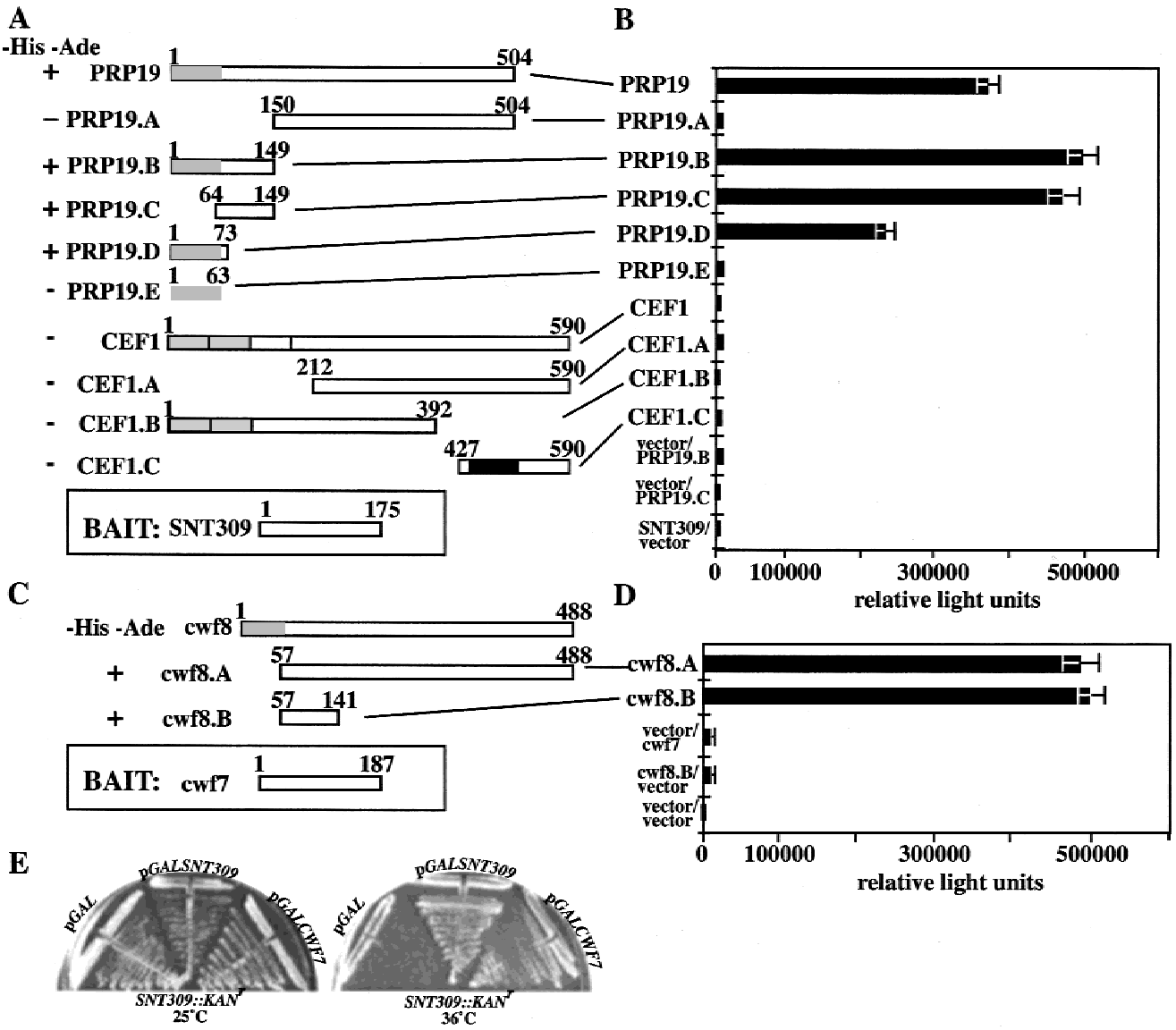

FIGURE 3. Interaction of *Sc* Snt309p and its *S. pombe* homolog, Cwf7p, with Prp19p/Cwf8p. **A:** The PJ69-4A strain was transformed with pGBT9SNT309 and pGAD424 carrying PRP19, PRP19.A, PRP19.B, PRP19.C, PRP19.D, CEF1, CEF1.A, CEF1.B, or CEF1.C, which are shown schematically. Shaded portions are as described in Figure 1A,C, with the exception of the black box in Cef1p, which represents the Prp19p binding domain. + denotes growth and − denotes no growth on selective media. **B:** β-galactosidase activity (represented by relative light units) of the strains described in **A**. **C:** The PJ69-4A strain was transformed with pGBT9CWF7 and pGAD424 carrying one of the *CWF8* fragments CWF8.A or CWF8.B, which are shown schematically. Shaded portions are as described in Figure 1A,C. + denotes growth and − denotes no grow on selective media. **D:** β-galactosidase activity (represented by relative light units) of the strains described in **C**. **E:** cDNAs encoding *Sc SNT309* and *Sp cwf7*$^+$ were placed under the control of the *GAL1* promoter in a 2-μm plasmid. Empty plasmid (p*GAL1*), p*GAL1SNT309*, or p*GAL1cwf7*$^+$ were transformed into the *SNT309*Δ strains and struck to medium lacking glucose at 25 °C and 36 °C and checked for growth after 5 days.

Evidence that Prp19p interacts with Cwc2p

In addition to Cef1p (Ntc85p) and Snt309p (Ntc25p), Prp19p binds a 40-kDa protein (Ntc40p) by far western analysis (Tarn et al., 1994) whose identity has not yet been reported. Based on its predicted molecular weight, we reasoned that *Sc* Cwc2p might represent Ntc40p. This possibility was first tested by two-hybrid analysis, and satisfyingly, full-length Cwc2p was found to interact with Prp19p. The association region in Cwc2p was further mapped to amino acids 228–340 in the C-terminus (Fig. 5A,B). Cwc2p, an essential protein of previously undescribed function, contains an RNA recognition motif (RRM; residues 159–168 and 194–203) that is known to facilitate both protein–RNA and protein–protein interactions (Shamoo et al., 1995; Sakashita & Sakamoto, 1996; Samuels et al., 1998). The Prp19p-binding segment is distinct

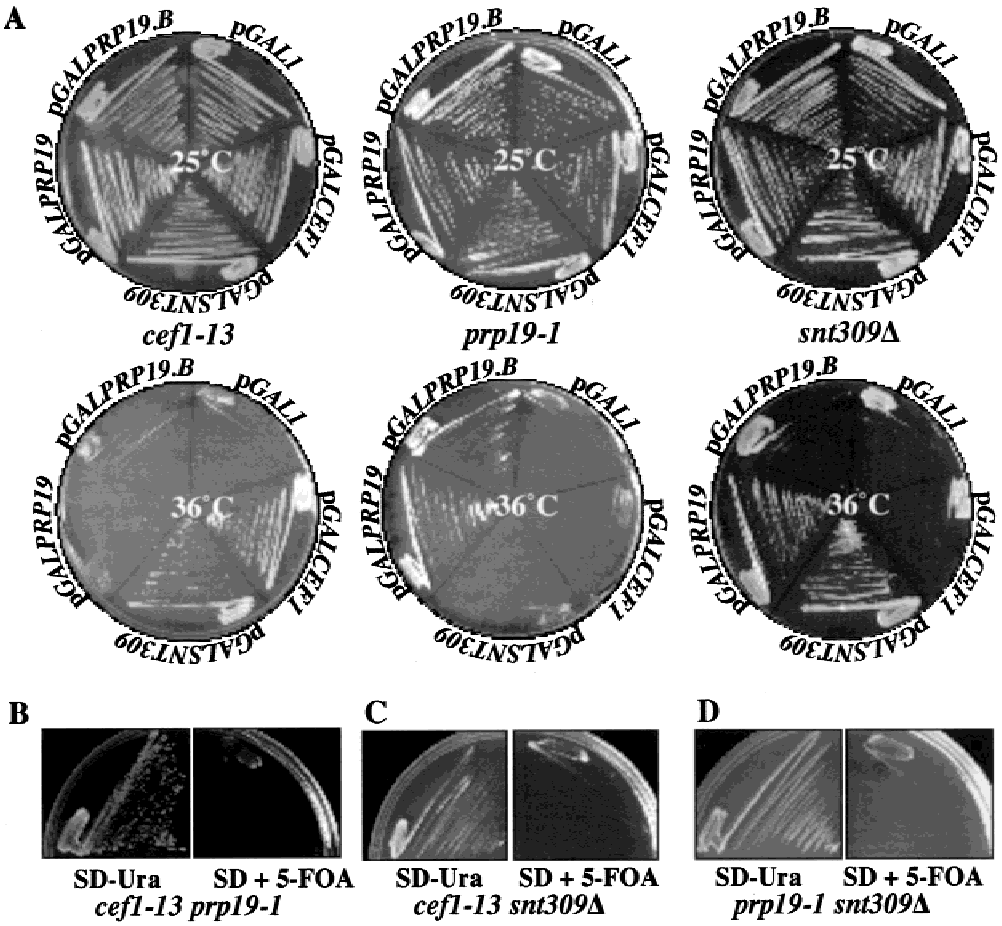

FIGURE 4. Genetic interactions between *CEF1*, *PRP19*, and *SNT309*. **A:** cDNAs encoding *CEF1*, *SNT309*, *PRP19*, and PRP19.B were placed under the control of the *GAL1* promoter in a 2-μm plasmid. Empty plasmid (p*GAL1*), p*GAL1CEF1*, p*GAL1SNT309*, p*GAL1PRP19*, or p*GAL1PRP19*.B were transformed into the *cef1-13*, *prp19-1*, or SNT309Δ strains and struck to medium lacking glucose at 25 °C and 36 °C and checked for growth after 5 days. **B:** *cef1-13* and *prp19-1* are synthetically lethal. A *cef1-13 prp19-1* double mutant strain expressing *CEF1* from a *URA3*-based plasmid was struck to SC-Ura (left panel) or SC+Ura+5-FOA (right panel) and incubated for 3 days at 25 °C. **C:** *cef1-13* and *SNT309*Δ are synthetically lethal. A *cef1-13 SNT309*Δ double mutant strain expressing *CEF1* from a *URA3*-based plasmid was struck to SC-Ura (left panel) or SC+Ura+5-FOA (right panel) and incubated for 3 days at 25 °C. **D:** *SNT309*Δ and *prp19-1* are synthetically lethal. A *prp19-1 SNT309*Δ double mutant strain expressing *PRP19* from a *URA3*-based plasmid was struck to SC-Ura (left panel) or SC+Ura+5-FOA (right panel) and incubated for 3 days at 25 °C.

from the RRM domain. The region within Prp19p required for Cwc2p interaction was also narrowed. A C-terminal segment of Prp19p spanning amino acids 150 to 504 (PRP19.A) interacted with Cwc2p, whereas the N-terminal segments did not (Fig. 5C,D). Therefore it is most likely that the Cwc2p-binding site in Prp19p is located downstream of the Cef1p-binding site but upstream of the first WD40 repeat (Prp19p ~140–219; see alignment Fig. 2). To test whether Cwc2p and Prp19p might interact directly, we produced a MBP-Cwc2p 228–340 fusion protein and determined that it, but not MBP alone, could bind to in vitro-translated labeled Prp19p (Fig. 5E). From these data, Cwc2p most likely represents Ntc40p.

Based on the interaction with Prp19p, we would expect Cwc2p to be important for pre-mRNA splicing. To test this, we engineered a heat-inducible degron mutant, *cwc2-td*, by fusing a degron cassette to the N-terminus of Cwc2p (Dohmen et al., 1994; Labib et al., 1999). *cwc2-td* cells did not divide after being placed at the restrictive temperature (data not shown). After 1 h at the restrictive temperature, there was an accumulation of *DYN2* pre-mRNA in *cwc2-td* cells (Fig. 5F). These data indicate that *Sc* Cwc2p is likely to be involved in pre-mRNA splicing.

Further evidence that *Sc* Cwc2p is important for pre-mRNA splicing comes from work with *Sp cdc5-120*. *Sp cdc5-120* displayed a negative genetic interaction with *Sp prp3-1* (Potashkin et al., 1998; not to be confused with *Sc PRP3* that encodes an unrelated protein) but not with numerous other *prp* mutants (data not shown). We cloned a gene fragment that rescued *prp3-1*, determined it corresponded to the mutant gene by integration mapping (data not shown), and found by DNA

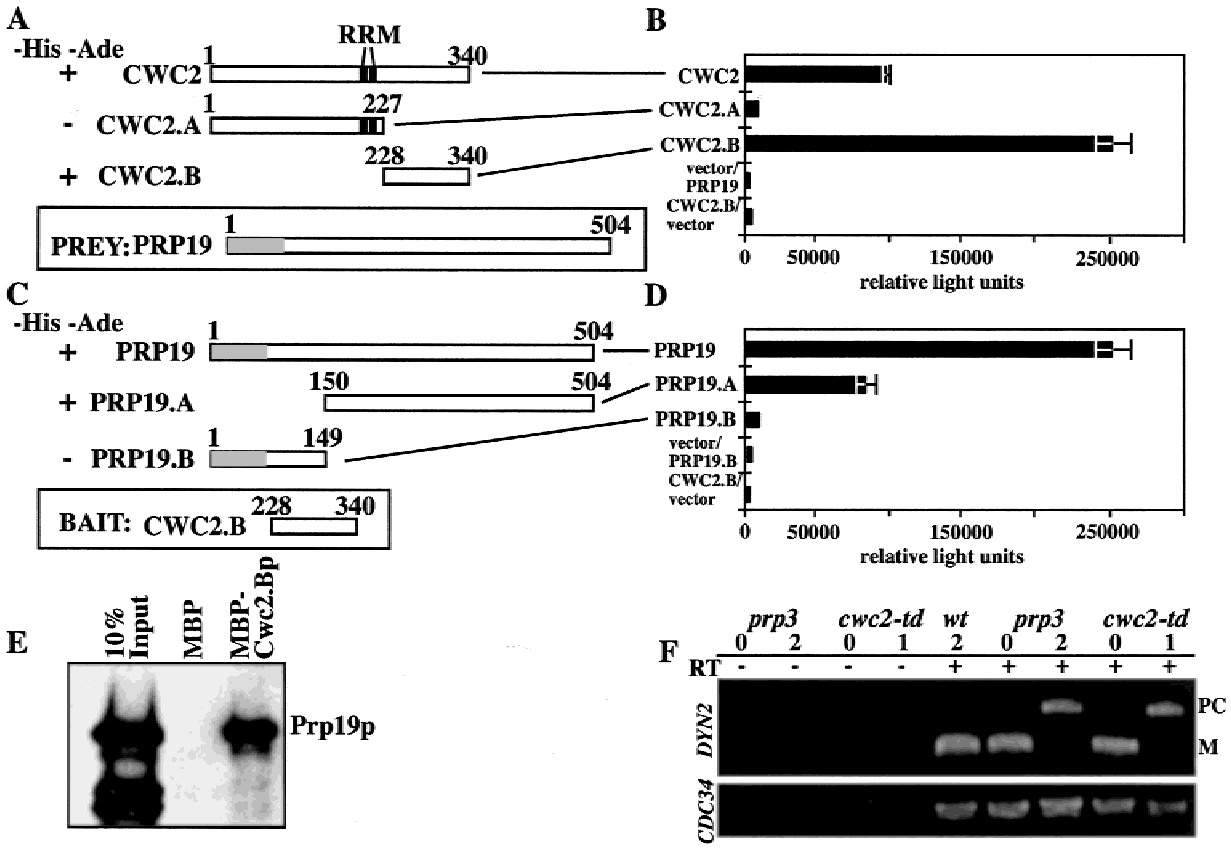

FIGURE 5. Cwc2p interacts with Prp19p. **A:** The PJ69-4A strain was transformed with pGAD424PRP19 and pGBT9 carrying CWC2, CWC2.A, or CWC2.B, which are shown schematically. Shaded portions represent the RRM domain. + denotes growth and − denotes no grow on selective media. **B:** β-galactosidase activity (represented by relative light units) of the strains described in **A**. **C:** The PJ69-4A strain was transformed with pGBT9CWC2.B and pGAD424 carrying PRP19, PRP19.A, PRP19.B, or PRP19.C, which are shown schematically. Shaded portion represents the U-box domain. + denotes growth and − denotes no growth on selective media. **D:** β-galactosidase activity (represented by relative light units) of the strains described in **C**. **E:** MBP or MBP-Cwc2p 228–340 (Cwc2.B) bound to amylose beads were mixed with in vitro-translated Prp19p. After extensive washes, the proteins were resolved by SDS-PAGE and autoradiography. "Input" represents a sample (1/10) of in vitro-translated Prp19p added to the binding reaction. **F:** RT-PCR analysis of *DYN2* and *CDC34* RNA isolated from *cwc2-td* cells grown at 37 °C for 0 or 1 h, *prp3-1* cells grown at 37 °C for 0 or 2 h, or wild-type cells grown at 37 °C for 2 h. −: reverse transcriptase was not added. +: reverse transcriptase was added. PC: precursor; M: mature.

sequence analysis that it contained a single open reading frame corresponding to *cwf2*$^+$ (the *S. pombe* homolog of *CWC2*). Thus, *cwf2*$^+$ is allelic with *prp3*$^+$. Because the *prp3-1* mutant accumulates pre-mRNAs at restrictive temperature (Potashkin et al., 1998), these observations suggest that both *Sp* Cwf2p and *Sc* Cwc2p are involved in pre-mRNA splicing.

Evidence that Cef1p interacts with Prp46p

prp5-1 and *cdc5-120* showed a strong negative genetic interaction, suggesting that these proteins might interact physically (McDonald et al., 1999). This coupled with the predicted molecular weight of *Sp* Prp5p and its *S. cerevisiae* homolog Prp46p led us to propose that *Sc* Prp46p might represent Ntc50p (Ohi et al., 2002). Further evidence supporting this conclusion came from sucrose gradient analyses of the *Sp* Cwf complex in the *cdc5 -ts*Δ*C* mutant background. These cells express a C-terminally truncated form of Cdc5p and are temperature sensitive for growth. *Sp* Prp5p but not *Sp* Cwf8p dissociated from the 40S Cdc5p-containing complex in these cells at the restrictive temperature (W.H. McDonald & K.L. Gould, unpubl. observation), suggesting that the C-terminus of *Sp* Cdc5p might interact with *Sp* Prp5p. Thus, we asked whether the *S. cerevisiae* homolog of *Sp* Prp5p, Prp46p, would interact with Cef1p in the two-hybrid assay. Indeed, full-length *Sc* Cef1p and C-terminal Cef1p fragments supported the Prp46p interaction (Fig. 6A,B).

Homologs of *Sp* Prp5p share significant sequence identity throughout their entire lengths and contain four WD40 repeats. A fragment of *Sc* Prp46p containing all four WD40 repeats (PRP46.C) was sufficient to support interaction with Cef1p, whereas an N-terminal segment (PRP46.A) did not (Fig. 6C,D). We have not

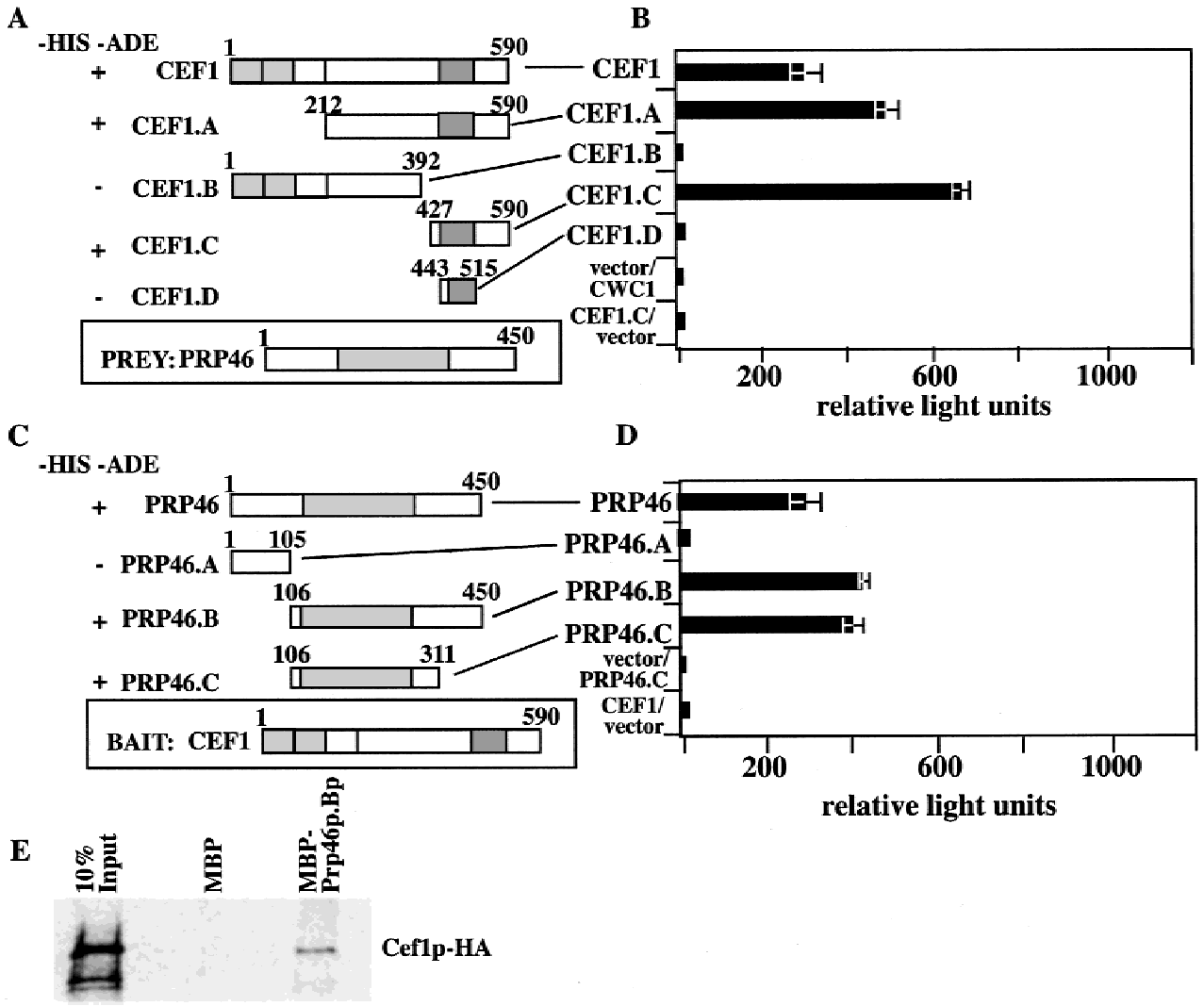

FIGURE 6. Prp46p interacts with Cef1p. **A:** The PJ69-4A strain was transformed with pGAD424PRP46 and pGBT9 carrying CEF1, CEF1.A, CEF1.B, CEF1.C, or CEF1.D, which are shown schematically. Light shaded portions represent the R1 and R2 Myb repeats, the open box depicts MLR3, and the dark shaded region represents the Prp19p binding region in Cef1p. **B:** β-galactosidase activity (represented by relative light units) of the strains described in **A**. **C:** The PJ69-4A strain was transformed with pGBT9CEF1 and pGAD424 carrying PRP46, PRP46.A, PRP46.B, PRP46.C or PRP46.D, which are shown schematically. Shaded portion represents the four WD40 domains. + denotes growth and − denotes no growth on selective media. **D:** β-galactosidase activity (represented by relative light units) of the strains described in **C**. **E:** MBP or MBP-Prp46p 106–450 (Prp46.B) bound to amylose beads were mixed with in vitro-translated Cef1p-HA. After extensive washes, the proteins were resolved by SDS-PAGE and autoradiography. "Input" represents a sample (1/10) of in vitro-translated Cef1p-HA added to the binding reaction.

tested which WD40 repeat(s) is required for this interaction.

To test whether these proteins might interact directly, an in vitro binding assay was performed. MBP-Prp46p 106–450, but not MBP alone, bound to labeled in vitro-translated Cef1p-HA (Fig. 6E). This interaction between Prp46p and Cef1p strongly suggests that *Sc* Prp46p represents Ntc50p.

Evidence that Syf1p interacts with Cef1p

We proposed that *Sc* Syf1p might represent Ntc90p (Ohi et al., 2002). This possibility was tested by examining protein–protein interactions between Syf1p and other Ntc components using two-hybrid analysis. Satisfyingly, Syf1p interacted with Cef1p, Ntc20p, Ntc30p/Isy1p, Syf1p, Clf1p, and Prp46p (Ntc50p) (Fig. 7A,B,F), suggesting that Syf1p represents Ntc90p.

Syf1p homologs exist in a variety of organisms (*Sp* Cwf3p, Q9P7R9; *Human* AAH07208; *D. melanogaster* Q9V6S4; and *C. elegans* P91175). The SYF1 family of proteins share significant sequence identity throughout their entire lengths and contain a series of nine tetratricopeptide repeats (TPR) most similar to *D. melanogaster* crooked neck (*crn*; Zhang et al., 1991; Verhasselt & Volckaert, 1997; Ben-Yehuda et al., 2000a). A fragment

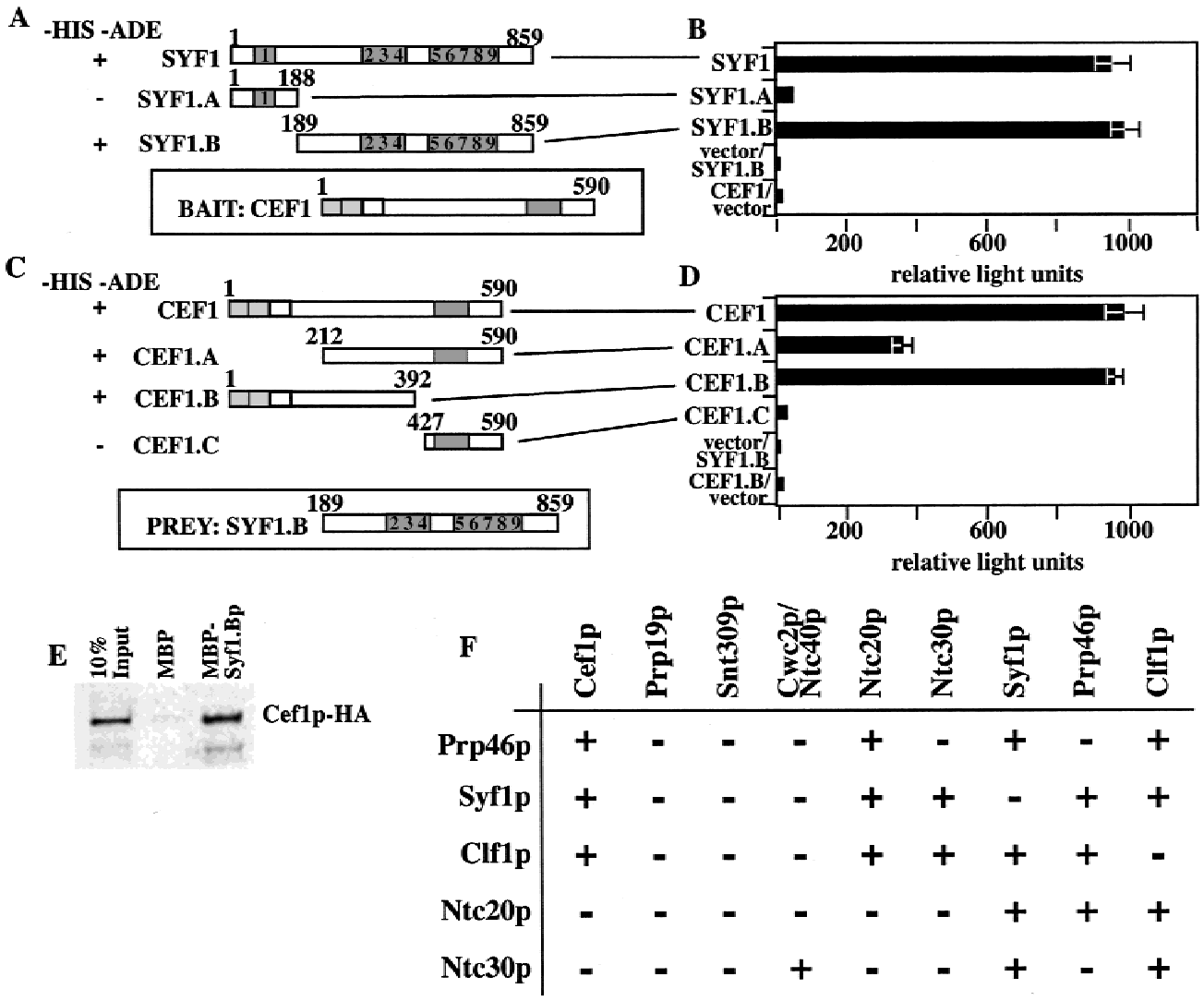

FIGURE 7. Protein–protein interactions mapped between Ntc components. **A:** The PJ69-4A strain was transformed with pGBT9424CEF1 and pGAD424 carrying SYF1, SYF1.A, or SYF1.B, which are shown schematically. Shaded boxes represent the TPR motifs. + denotes growth and − denotes no growth on selective media. **B:** β-galactosidase activity (represented by relative light units) of the strains described in **A**. **C:** The PJ69-4A strain was transformed with pGAD424SYF1.B and pGBT9 carrying CEF1, CEF1.A, CEF1.B, or CEF1.C, which are shown schematically. Light shaded portions represent the R1 and R2 Myb repeats, the open box depicts MLR3, and the dark shaded region represents the Prp19p binding region in Cef1p. + denotes growth and − denotes no growth on selective media. **D:** β-galactosidase activity (represented by relative light units) of the strains described in **C**. **E:** MBP or MBP-Syf1p 189–859 (Syf1.B) bound to amylose beads were mixed with in vitro-translated Cef1p-HA. After extensive washes, the proteins were resolved by SDS-PAGE and autoradiography. "Input" represents a sample (1/10) of in vitro-translated Cef1p-HA before the binding reaction. **F:** Summary of two-hybrid interactions found between Ntc components Prp46p, Syf1p, Clf1p, Ntc20p, and Ntc30p with Cef1p, Prp19p, Snt309p, Cwc2p, Ntc20p, Ntc30p, Syf1p, Prp46p, and Syf1p. + denotes growth and − denotes no growth on selective media.

of Syf1p containing a majority of the TPR repeats (SYF1.B) was sufficient to support interaction with Cef1p, Ntc20p, Syf1p, Clf1p, and Prp46p, whereas an N-terminal segment (SYF1.A) did not (Fig. 7A,B,F; data not shown). However, the N-terminal segment of Syf1p containing TRP1 (SYF1.A) was sufficient to support interaction with Ntc30p/Isy1p (data not shown). We have not examined which TPR(s) repeats in the C-terminus are required to support the individual interactions between Syf1p and Cef1p, Ntc20p, Syf1p, Clf1p, or Prp46p. It is most likely that some of these interactions will require other Cwc members.

To define the Syf1p binding region in Cef1p, we tested a series of *CEF1* constructs for their ability to support interaction with SYF1.B in the two-hybrid system (Fig. 7C,D). SYF1.B interacted with both CEF1.A and CEF1.B but not with CEF1.C (Fig. 7C,D) Therefore Syf1p interacts with the region of Cef1p downstream from the Myb repeats but upstream of both the Prp46p and Prp19p binding regions. To test if this

might be direct, an in vitro binding assay was performed with Syf1p. MBP-Syf1p 189–859, but not MBP alone, bound to labeled in vitro-translated Cef1p-HA (Fig. 7E).

To further delineate the molecular architecture of the Ntc complex, all possible interactions between Cef1p, Prp19p, Snt309p, Cwc2p (Ntc40p), Prp46p (Ntc50p), Syf1p (Ntc90p), Clf1p (most likely Ntc77p), Ntc30p, and Ntc20p were examined. Figure 7F summarizes these results. The molecular weight of Clf1p and its ability of to interact with Cef1p, Ntc20p, Ntc30p, Syf1p (Ntc90p), and Prp46 (Ntc50p) make it likely that Clf1p represents Ntc77p.

The *prp19-1* mutation disrupts important protein–protein interactions

The mutation in Prp19-1p lies in the conserved U-box motif and results in the substitution of an isoleucine for the conserved valine at position 14 (Chen et al., 1998). Because this domain is not required for interactions between Prp19p–Cef1p or Prp19p–Snt309p, we predicted that Cef1p and Snt309p would still be able to interact with the Prp19-1p mutant. However, neither *CEF1.C* nor *SNT309* could interact with *prp19-1* or *prp19-1.B* (Fig. 8A,B). One explanation for these results would be that Prp19-1p is an unstable protein. To examine this possibility, the *prp19-1* locus was engineered to encode a protein with a C-terminal myc epitope tag. The addition of this tag did not interfere with the strain's growth at 25 °C and Prp19-1p-myc still associated with Cef1p at 25 °C (data not shown). To examine the temperature-sensitive phenotype of this strain, *PRP19-myc*, *prp19-1*, and *prp19-1-myc* strains were grown to mid-log phase at 25 °C and shifted to the restrictive temperature. After 4 h, *prp19-1-myc* cell numbers stopped increasing whereas *PRP19-myc* cells continued to divide exponentially and *prp19-1* cells doubled at least twice (Fig. 8C). Therefore, the myc tag appears to exacerbate the temperature sensitivity of Prp19-1p. However, Prp19-1p-myc levels remained constant throughout the experiment (Fig. 8D), indicating that the mutant protein is not thermosensitive.

We examined the interactions of Cef1p, Snt309p, and Cwc2p with each other and with the complex in vivo in the prp19-1 mutant. To analyze Cef1p levels, we raised polyclonal antibodies and tested their specificity by immunoblotting. From wild-type cells, the anti-Cef1p serum recognized a single band of expected size (68 kDa; Fig. 8E). From a strain in which the *CEF1* locus was engineered to encode Cef1p-myc, a single band was again recognized that corresponded to the predicted increase in molecular mass attributable to the epitope tag (Fig. 8E). Finally, the ~68 kDa band was recognized in lysates from *CEF1* null cells covered by p*GAL1CEF1* in the absence of glucose (*GAL1* promoter on), but not in the presence of glucose (*GAL1* promoter off; Fig. 8E). Using these specific antibodies, Cef1p levels were examined in the *prp19-1* strain and found to be reduced at permissive temperature, difficult to detect at 2 h into the time course, and undetectable at 4 h into the time course (Fig. 8F). Snt309p-myc levels decreased somewhat throughout the experiment but remained at detectable levels (Fig. 8F). Cwc2p-myc levels remained constant throughout the experiment (Fig. 8F).

To determine if these proteins were still associated with a high molecular weight complex in *prp19-1* cells, we examined the sedimentation characteristics of Snt309p-myc and Cwc2p-myc in *prp19-1* strains after 0, 2 and 8 h at restrictive temperature. When isolated from *prp19-1* cells grown at 25 °C, these proteins sedimented primarily in two regions of the gradient (Fig. 8G), similar to what we observed with Cef1p-myc and Prp19p-myc (data not shown). In a *prp19-1* grown at the restrictive temperature for 2 and 8 h, however, these proteins were de-

FIGURE 8. Characterization of *prp19-1*. **A:** The PJ69-4A strain was transformed with pGBT9 carrying the *CEF1* fragment CEF1.C or SNT309 and pGAD424 carrying either PRP19.B or *prp19-1*.B, which are shown schematically. Shaded portions are as described in Figure 1C. An asterisk depicts the location of the mutation found in *prp19-1*. **B:** β-galactosidase activity (represented by relative light units) of the strains described in **A**. **C:** Exponentially growing *PRP19-myc* (KGY1604), *prp19-1* (KGY1811), and *prp19-1myc* cells (KGY1655) were shifted to 36.0 °C at $t = 0$ and samples collected at 2-h intervals to determine cell number. Filled diamonds: *PRP19-myc*; filled squares: *prp19-1*; filled triangles: *prp19-1myc*. **D:** Lysate from *prp19-1myc* (KGY1655) was probed with anti-myc and anti-PSTAIR antibodies after 0, 2, 4, 6, and 8 h at 36 °C. **E:** Characterization of affinity-purified Cef1p antibodies (VU136#9). An immunoblot of straight lysates from wild-type (YPH98) cells (lane 1), Cef1-myc (KGY1601) cells (lane 2), and from *CEF1* null cells covered by p*GAL1CEF1* (KGY1120; Ohi et al., 1998) in the absence (−, *GAL1* promoter on) or presence (+; *GAL1* promoter off) of glucose. **F:** Lysates from *CWC2-myc* (KGY1606), *SNT309-myc* (KGY2401), *SNT309-myc prp19-1* (KGY1997), and *CWC2-myc prp19-1* (KGY2406) were probed with anti-Cef1p, anti-myc, and anti-PSTAIR antibodies after 0, 2, 4, 6, and 8 hours at 36 °C. **G:** Snt309p-myc and Cwc2p-myc do not sediment in a large complex in the *prp19-1* background. Immunoblots on fractions from 10–30% sucrose gradients. Lysates from *SNT309-myc prp19-1* (KGY1997) and *CWC2-myc prp19-1* (KGY2406) after 0, 2, and 8 h at 36 °C probed with anti-9E10 antibodies. The migration of FAS (40S), thyroglobulin (19S), and catalase (11.3S) collected from parallel gradients is indicated. **H:** Prp46p, Syf1p, and Clf1p no longer sediment in large complexes in the *prp19-1* background. Immunoblots on fractions from 10–30% sucrose gradients. Lysates from *PRP46-myc prp19-1* (KGY2078), *SYF1-myc prp19-1* (KGY1659), and *CLF1-myc prp19-1* (KGY1660) after 0, 2, and 8 h at 36 °C probed with anti-9E10 antibodies. The migration of FAS (40S), thyroglobulin (19S), and catalase (11.3S) collected from parallel gradients is indicated.

tected primarily near the top of the gradient (Fig. 8G). We also examined the sedimentation characteristics of Prp46p (Ntc50p), Syf1p (Ntc90p), and Clf1p (Ntc77p). Prp46p, Syf1p-myc, and Clf1p-myc levels remained constant throughout the temperature shift (data not shown) and sedimented in two regions of the gradient when isolated from *prp19-1* cells grown at 25 °C (Fig. 8H). However, in *prp19-1* cells grown at the restrictive temperature, Prp46p-myc, Syf1p-myc, and Clf1p-myc are less abundant at the high molecular weight fractions at 2 h and sediment near the top of the gradient by 8 h (Fig. 8H). We conclude that a mutation in the U-box of Prp19p disrupts the integrity of the Ntc subcomplex and leads to Cef1p degradation.

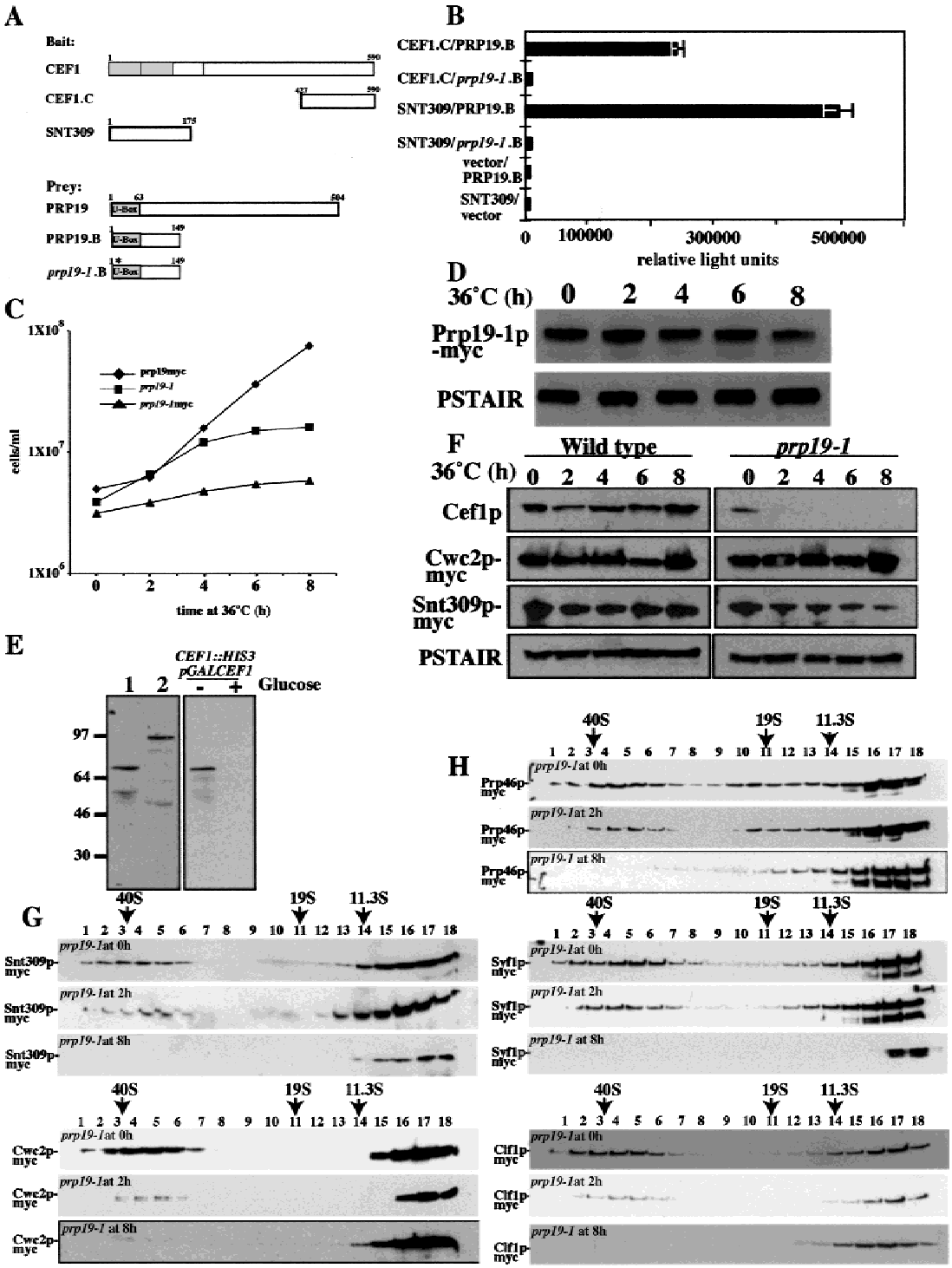

FIGURE 8. (*See caption on facing page.*)

DISCUSSION

In this study, we have concentrated on mapping genetic and physical interactions involving Cef1p, its binding partner, Prp19p, and other components of the Ntc. We identified four conserved proteins that interact with Cef1p or Prp19p, suggesting that they represent previously uncharacterized Ntc components, mapped important interactions between these and known Ntc proteins (summarized in Fig. 9A), and demonstrated an involvement of one such uncharacterized protein, Cwf2p/Cwc2p, in pre-mRNA splicing. Ntc components exist within a larger complex that contains the U2, U5, and U6 snRNAs (Ohi et al., 2002) and are also found in the penta-snRNP (Stevens et al., 2002). However, the Ntc has been isolated as a distinct unit, indicating that its constituents bind directly with one another (Tarn et al., 1994; Chen et al., 1998, 2001; Tsai et al., 1999). Although this property of these *S. cerevisiae* splicing factors has been useful for the purpose of mapping protein–protein interactions, we note that there is no evidence for the existence of this smaller protein unit in fission yeast; *Sp* Cdc5p has only been detected within a larger complex that contains snRNAs (McDonald et al., 1999; Ohi et al., 2002).

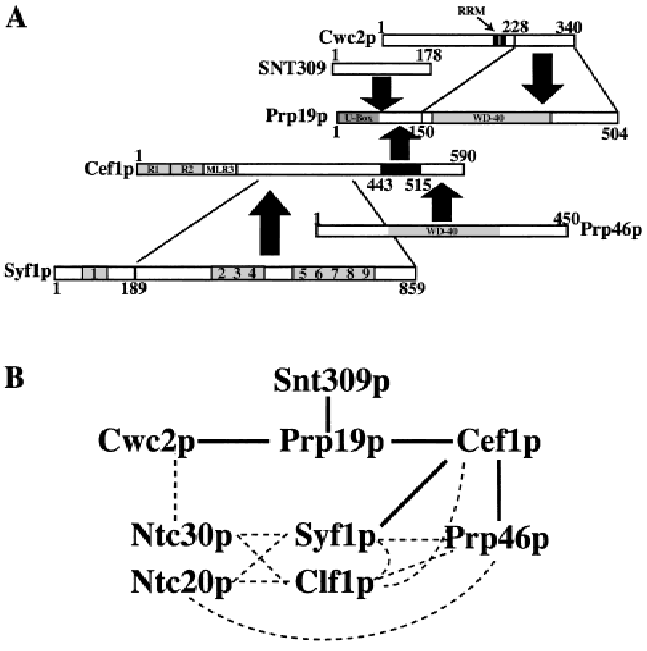

FIGURE 9. Protein–protein interactions among members of the Ntc. **A:** Summary of regions found to support protein–protein interactions in two-hybrid and in vitro binding assays. Shaded arrows represent in vitro binding results. **B:** Model of protein–protein interactions mapped between Cef1p, Prp19p, Snt309p, Cwc2p, Ntc20p, Ntc30p, Syf1p, Prp46p, and Syf1p. Solid lines represent protein–protein interactions detected by in vitro binding assays and far western analysis (Chen et al., 1999; Tsai et al., 1999). Dotted lines represent protein–protein interactions found by two-hybrid analysis.

Identified Ntc members included Prp19p (the founding member of the complex), Cef1p (Ntc85p), Snt309p (Ntc25p), Syf2p (Ntc31p), Isy1p (Ntc30p), and Ntc20p. We found that both Cef1p and Snt309p interact independently with residues 64–149 of Prp19p (Figs. 1 and 3). Consistent with this, we have uncovered many genetic interactions between mutations of the genes encoding Prp19p, Cef1p, and Snt309p (Fig. 4). These include synthetic lethal interactions between *cef1-13*, *snt309*Δ, and *prp19-1*, as well as the rescue of the temperature-sensitive phenotype of *cef1-13* by overexpression of *SNT309*. These data are consistent with the observation that Snt309p stabilizes Prp19p's interaction with other Ntc members (Chen et al., 1999). The 72-amino-acid region of Cef1p that binds Prp19p contains a 4-amino-acid EVES motif that was first identified in vertebrate c-Myb proteins (Dash et al., 1996). This motif mediates protein–protein interactions between Myb and interacting components, which raised the possibility that these residues may be important for Cef1p–Prp19p protein interaction. However, mutation of these amino acids, either separately or in combination, did not disrupt interaction between Cef1p and Prp19p (data not shown).

Because of the conservation found between the *Sc* Cwc and *Sp* Cwf spliceosomal complexes, we were puzzled by the observation that *S. pombe* and higher eukaryotes do not have obvious *Sc* Snt309p homologs. However, *Sp* Cwf7p was a similar molecular weight to *Sc* Snt309p and also, the mammalian homolog of *Sp* Cwf7p, SPF27, copurified with hCDC5 in a core of four proteins, suggesting it is closely associated with hCDC5 (Ajuh et al., 2000). For these reasons, we tested whether *Sp* Cwf7p might be a functional homolog of *Sc* Snt309p. Indeed, overexpression of *Sp cwf7*$^{+}$ cDNA rescued the *SNT309* null mutation. Moreover, *Sp* Cwf7p interacted with the same conserved sequence element of *Sp* Cwf8p that mediates *Sc* Snt309p interaction with *Sc* Prp19p. The observation that *Sp* Cwf7p and *Sc* Snt309p are functional homologs provides further evidence that spliceosomes from the two yeasts are organized in a similar manner.

Our results of an interaction between Cef1p and Prp46p complement those of Ajuh et al. (2001). The human homolog of *Sp* Prp5p and *Sc* Prp46p, hPRL1, was identified as a member of the mammalian spliceosome and a core component of the CDC5L complex (Neubauer et al., 1998; Ajuh et al., 2000). As in the case of yeast, the WD40 repeats of the human homolog interact with the C-terminus of hCDC5 (Ajuh et al., 2001). This interaction is not mutually exclusive, as Prp19p and Prp46p bind to distinct regions of Cef1p (compare Fig. 1A and Fig. 6A). In *S. pombe*, *cdc5-120* and *prp5-1* are synthetically lethal, providing further evidence that the interaction between these two proteins is evolutionarily conserved (McDonald et al., 1999).

We have shown that Cwc2p binds to Prp19p and is required for pre-mRNA splicing in vivo (Fig. 5) and that its *S. pombe* homolog, Cwf2p is allelic to *Sp* Prp3p, strongly suggesting that this 40-kDa protein represents the previously uncharacterized Ntc40p. These data extend the direct binding interactions observed in previous analyses of the Ntc complex (Tarn et al., 1994; Chen et al., 1998, 2002; Tsai et al., 1999).

To further delineate the molecular architecture of the Ntc complex, we examined all possible protein–protein interactions between Cef1p, Prp19p, Snt309p, Cwc2p (Ntc40p), Prp46p (Ntc50p), Syf1p (Ntc90p), Clf1p (most likely Ntc77p), Isy1p (Ntc30p), and Ntc20p using two-hybrid analysis. Figure 9B summarizes these results as well as in vitro binding interactions we detected. As indicated by the dotted lines, in vitro binding interactions were not always detected despite strong two-hybrid interactions. For example, MBP-Cwc2p was not able to bind to in vitro-translated Isy1p (Ntc30p), nor did MBP-Ntc20p bind to in vitro-translated Prp46p (data not shown). There are several possible explanations for such results. The first is that the two-hybrid interactions require a bridging protein(s). In this scenario, the tested proteins do not make direct contact with one another. The second possibility is that certain interactions might require separate interactions that provide stability to the one under examination. With the understanding that these proteins form a discrete complex, it is not difficult to imagine an interdependence of protein interactions. A third possibility is that posttranslational modifications of the proteins that do not occur in vitro may be required for binding.

Other groups have previously noted numerous two-hybrid interactions between Cef1p, Syf1p, Clf1p, Ntc30p/Isy1p, and Ntc20p (Ben-Yehuda et al., 1998, 2000b; Dix et al., 1998; Russell et al., 2000), although it has not been appreciated that these interactions occur within the context of a stable complex. Although we have not yet placed Ntc30p/Isy1p or Ntc20p within the complex, we have made significant progress in mapping protein interactions between identified and previously unidentified Ntc components. Interestingly, we have been unable to detect an interaction between Ntc30p/Isy1p and Cef1p that was reported by Ben-Yehuda et al. (2000b). Such an interaction was also not detected by far western analysis (Tsai et al., 1999; Chen et al., 2001). While our paper was under revision, complementary conclusions regarding the identity of Ntc77p as Clf1p and Ntc90p as Sylf1p were published by Chen et al. (2002). These authors also determined that Clf1p and Syf1p interacted with Cef1p, Ntc20p, and Isy1p (Ntc30p) by two-hybrid analysis.

Of significance to understanding Cdc5p/Cef1p function was our finding that a mutation in *PRP19* led to loss of Cef1p. This indicates that Cef1p/Cdc5p function depends on its interaction with Prp19p. In light of this finding, although a number of reports have suggested a role for hCDC5 in transcriptional regulation (Hirayama & Shinozaki, 1996; Bernstein & Coughlin, 1997, 1998; Groenen et al., 1998), it is likely that Cdc5p/Cef1p is involved primarily in pre-mRNA processing, as no transcriptional function has been attributed to Prp19p.

Of significance to understanding Prp19p function, we have found that Prp19p is required to maintain the organization of the Ntc unit, including Cef1p, Cwc2p, Snt309p, Prp46p, Syf1p, and Clf1p. These data, coupled with the recent observation that hNMP200, a nuclear matrix protein, represents hPRP19 (Gotzmann et al., 2000) suggests a role for Prp19p as a scaffolding protein. In this scenario, Prp19p, which is believed to have the ability to oligomerize (Cheng et al., 1993), would provide a platform for Cef1p, Snt309p, Cwc2p, and other components of the Ntc complex to organize upon. That proteins other than those described here bind Prp19p directly is likely, as no protein interactions have yet been mapped to its U-box or WD40 repeats.

The presence of the U-box in Prp19p raises the intriguing possibility that Prp19p is involved in protein ubiquitination. Originally characterized in *Sc* Ufd2p, the U-box domain has been predicted to adopt a RING-fold based on sequence-profile analysis (Koegl et al., 1999; Aravind & Koonin, 2000). Proteins containing RING domains have been shown to mediate the highly regulated step of substrate recognition in the ubiquitination cascade, facilitating the transfer of activated ubiquitin from the E2 to the substrate. In addition to marking a protein for proteolysis by the 26S proteosome, ubiquitination has also been shown to regulate other cellular processes (reviewed in Freemont, 2000; Jackson et al., 2000; Tyers & Jorgensen, 2000; Pickart, 2001). Although the structure of the U-box motif has yet to be solved, several U-box-containing proteins, including human PRP19, have been shown to act as E3 ligases in vitro (Koegl et al., 1999; Hatakeyama et al., 2001; Jiang et al., 2001). Because a mutation within the U-box (in Prp19-1p) disrupts the structure of the Ntc and pre-mRNA splicing, it will be interesting to determine if the U-box facilitates ubiquitination of Ntc complex members and what role such ubiquitination might play in pre-mRNA splicing.

MATERIAL AND METHODS

Strains and media

S. cerevisiae strains used in this study (Table 1) were grown either in synthetic minimal medium with the appropriate nutritional supplements or YPD (Guthrie & Fink, 1991). Transformations were performed by the lithium acetate method (Gietz et al., 1995). Yeast two-hybrid studies were done in *S. cerevisiae* strain PJ69-4A (KGY1296; James et al., 1996). *MAT* a *prp19-1* was backcrossed three times to YPH98 prior to analysis. For determination of cell numbers, samples were prepared and analyzed on a Coulter Multisizer II (Coulter Electronics Ltd., England) as described (Ohi et al., 1998).

TABLE 1. Strains used in this study.

Strain number	Relevant genotype	Source
KGY823	YPH98, *MAT*a *ura3*-52 *lys2*-801 *ade2*-101 *leu2*- Δ1 *trp1*- Δ1	Lab stock
KGY1296	PJ69-4A, *MAT*a; *trp1-190 lue2-3,112 ura3-52 his3-200 gal4 delete LYS2* replaced by *GAL1-HIS3 GAL2-ADE2, met2* replaced by *GAL-LacZ*	James et al. (1996)
KGY1604	*MAT*a *PRP19::PRP19-myc13*::KAN^r*ura3*-52 *lys2*-801 *ade2*-101 *leu2*- Δ1 *trp1*-Δ1	This study
KGY1606	*MAT*a *CWC2::CWC2-myc13*::KAN^r*ura3*-52 *lys2*-801 *ade2*-101 *leu2*- Δ1 *trp1*- Δ1	This study
KGY1614	*MATα cef1-13 ade2*-101 *ade3*Δ *ura3*-52 *lys2*-801 *trp1*-Δ63 *his3*-Δ200 *leu2*-Δ1	Ohi et al. (1998)
KGY1654	*cwc2-td; MATα CWC2::KAN^r ura3DO::CUPi-Ub-Arg-DHFRts-ha-CWC2::URA3 his3D1 leu2DO met15DO lys2 DO*	This study
KGY1655	*MAT*a *prp19-1::prp19-1 myc13*:: *KAN^r ura3*-52 *lys2*-801 *ade2*-101 *leu2*-Δ1 *trp1*-Δ1	This study
KGY1659	*MATα prp19-1 SYF1::SYF1-myc13::KAN^r*	This study
KGY1660	*MATα prp19-1 CLF1::CLF1-myc13::KAN^r*	This study
KGY1693	*MATa CEF1::CEF1-myc13::KAN^r PRP19::PRP19-HA*::KAN^r	This study
KGY1812	*MATα prp19-1 ura3*-52 *lys2*-801 *ade2*-101 *leu2*-Δ1 *trp1*-Δ1	J. Abelson
KGY1939	*MAT*a *cef1-13 prp19-1*/ pRS416*CEF1*	This study
KGY1997	*MATa prp19-1 SNT309::SNT309-myc13::KAN^r*	This study
KGY2002	*MATa SNT309::KAN^r his3*D1 *leu2* DO *met15* DO *ura3* DO	Research Genetics
KGY2003	*MAT*a *cef1-13 SNT309::HIS31*/ pRS416*CEF1*	This study
KGY2009	*MAT*a*prp19-1 SNT309::KAN^{r}1*/ pRS416*PRP19*	This study
KGY2078	*MATα prp19-1 PRP46::PRP46-myc13::KAN^r*	This study
KGY2406	*MATα prp19-1 CWC2::CWC2-myc13::KAN^r*	This study
KGY2410	*MAT*a *SNT309::SNT309-myc13*::KAN^r *ura3*-52 *lys2*-801 *ade2*-101 *leu2*-Δ1 *trp1*-Δ1	This study
KGY2446	*MATα SNT309::HIS3 ura3*-52 *lys2*-801 *ade2*-101 *leu2*-Δ1 *his3*-Δ200	This study

Gene disruptions and shut-off strain

Deletion of the *SNT309* coding sequence was performed by replacing the entire ORF with the *HIS3* gene as described previously (Ohi et al., 1998) and confirmed by PCR. A separate *snt309*Δ strain was obtained from Research Genetics (Huntsville, Alabama). Both were utilized to confirm the synthetic lethality of *snt309*Δ *prp19-1.*

To construct *cwc2-td*, *CWC2* cDNA was used to replace the *Hin*dIII fragment of pPW66R (Dohmen et al., 1994). The resulting plasmid was linearized with *Pst*1 and integrated at the *ura3* locus of a diploid with one copy of the *CWC2* gene replaced with *HIS3*. Tetrad dissection was used to produce a strain in which the only functional copy of the *CWC2* gene was expressed from the copper-inducible *CUP1* promoter, with the temperature-sensitive degron cassette in frame at the 5′ end. *cwc2-td* was grown in medium containing 0.1 mM $CuSO_4$ at 25 °C. $CuSO_4$ was omitted from the medium when cells were shifted to 37 °C to induce degradation of the degron-fusion protein.

Molecular biology techniques

S. cerevisiae and *S. pombe* genomic DNA were isolated as described (Berry et al., 1999; Burns et al., 1999). Sequencing reactions were performed using Thermosequenase radiolabeled terminator cycle sequencing kit according to the manufacturer's instructions (Amersham Pharmacia Biotech). PCR amplifications were performed using *Pfu* turbo (Stratagene, La Jolla, California) according to the manufacturer's instructions.

Cloning and sequencing of *cwf7$^+$*

Oligonucleotide primers were used to amplify the *cwf7*$^+$ cDNA from a pDB20-based cDNA library (Fikes et al., 1990). Primer cwf7 5′Nde (TAGCATATGATGAGTTATAATATATCTTTGG) was complementary to the 5′ end of the cDNA, and primer cwf7 3′Bam (TAGGGATCCTTATGACAAGAGAGTAGC) was complementary to the 3′ end of the cDNA. The 5′ and 3′ primers were engineered to add a *Nde*1 site to the 5′ end of the coding region and a *Bam*H1 to the 3′ end of the coding region, respectively. The amplified cDNA was subcloned into pCRBlunt (Stratagene) and sequenced to ensure the absence of PCR-induced mutations.

Immunoprecipitations, immunoblots, and sucrose gradients

Denatured and native protein lysates were prepared as detailed previously (Gould et al., 1991). Immunoprecipitations with anti-HA (12CA5) or anti-myc (9E10) monoclonal antibodies were performed as described (McDonald et al., 1999). Proteins were resolved by SDS-PAGE on 6–20% gradient gels or on Novex NuPAGE 4–12% Bis-Tris gels using NuPAGE MOPS SDS running buffer (Invitrogen, Carlsbad, California). For immunoblotting, proteins were transferred by electroblotting to PVDF membrane (Immobilon P; Millipore Corp., Bedford, Massachusetts). Anti-Cdc5p serum JAM (McDonald et al., 1999) was used at 1:10,000 dilution. Affinity purified anti-Cef1p serum VU136#9 was used at an appropriate dilution. Anti-FAS antibodies, anti-HA (12CA5)

antibodies, and anti-myc (9E10) antibodies were used as described (McDonald et al., 1999). PSTAIRE antibodies (Sigma-Aldrich) were used at a dilution of 1:5,000. Antibodies were detected using horseradish peroxidase conjugated goat anti-rabbit or goat anti-mouse secondary antibodies (0.8 mg/mL; Jackson Immunoresearch Laboratories, West Grove, Pennsylvania) at a dilution of 1:50,000. Immunoblots were visualized using ECL reagents (Amersham Pharmacia Biotech). Sucrose gradients were done exactly as described previously (McDonald et al., 1999).

Yeast two-hybrid assays

The yeast two-hybrid system used in this study was described previously (James et al., 1996). Various portions of the *CEF1*, *PRP19*, *SNT309*, YDL209C (now termed *CWC2*), YPL151C (now termed *PRP46*), *SYF1*, *CLF1*, *NTC30*, *NTC20*, *cwf8*$^+$, and *cwf7*$^+$ cDNAs were cloned into the bait plasmid pGBT9 and/or the prey plasmid pGAD424 (Clonetech, Palo Alto, California) and sequenced to ensure the absence of PCR-induced mutations and that the correct reading frame had been retained.

Two-hybrid screens were performed as described (James et al., 1996). To test for protein interactions, both bait and prey plasmids were cotransformed into *S. cerevisiae* strain PJ69-4A. β-galactosidase reporter enzyme activity in the two-hybrid strains was measured using the Galacto-Star™ chemiluminescent reporter assay system according to the manufacturer's instructions (Tropix Inc., Bedford, Massachusetts), with the exception that cells were lysed by glass bead disruption. Each sample was measured in triplicate. Reporter assays were recorded either on the BMG luminometer (Bartlett-Williams Scientific, Chapel Hill, North Carolina) or the Mediators PhL luminometer (Aureon Biosystems, Vienna, Austria).

Expression of recombinant fusion proteins and in vitro binding assays

pGEX2TCEF1 427–590 (pKG1788) was constructed by subcloning an *Eco*RI-*PstI* fragment from pGBT9CEF1 427–590 (pKG1752) into pGEX2T (Amersham Pharmacia Biotech). pRSET(A)PRP19 1–149 (pKG211) and pMAL-c2PRP19 1–149 (pKGY95) were constructed using pCR-Blunt PRP19 (pKG1190) as a template for PCR amplification. The 5′Prp19.1(*Bam*H1) primer introduced a *BamH1* site and 3′Prp19.149 primer introduced a *Pst*1 site. This *PRP19* fragment was ligated into pRSET-A (Invitrogen) or pMAL-c2 (New England BioLabs, Beverly, Massachusetts) cut with *Bam*H1 and *Pst*1. pMAL-c2PRP46 106–450 (pKG557), pMAL-c2CWC2 228–340 (pKG311) was constructed using genomic DNA as a template for PCR amplification. The 5′Prp46.106(*EcoR1*) primer introduced a *Eco*R1 site and 3′Prp46.end primer introduced a *Sal*1 site. The 5′Cwc2.228(*Xmn*1) primer introduced a *Xmn*1 site and 3′Cwc2.340 primer introduced a *Pst*1 site. The *PRP46* and *CWC2* fragments were ligated into pMAL-c2 (New England BioLabs) cut with *Eco*R1/*Sal*1 or *Xmn1*/*Pst*1, respectively. pMAL-c2SYF 189–859 (pKGY1065) was constructed by subcloning an *Eco*R1-*Pst*1 fragment from pGBT9SYF1 189–859 (pKG859) into pMAL-c2. Recombinant fusion proteins were produced in bacterial cells after induction with 0.4 mM isopropyl-β-*D*-thiogalactopyranoside (IPTG). GST and GST-Cef1p 427–590 were purified according to standard methods (Frangioni & Neel, 1993). His^6-Prp19p 1-149 was purified from bacterial lysates under native conditions using Ni^{2+}-NTA resin as specified by the manufacturer (Qiagen, Valencia, California). MBP, MBP-Prp19p 1-149, MBP-Prp46p 106–450, MBP-Cwc2p 228–340, and MBP-Syf1p 189–859 were purified using Amylose resin according to the manufacturer's instructions (New England BioLabs).

pSK(+)PRP19 (pKG1781) and pRS414CEF1-3XHA (pKG1875) were translated in vitro in the presence of ^{35}S-Trans label (ICN Pharmaceuticals, Irvine, California) with the use of the T_NT coupled reticulocyte lysate system (Promega, Madison, Wisconsin). Purified GST or GST-Cef1p 427–590 bound to glutathione-agarose beads were mixed with ^{35}S-labeled Prp19p in binding buffer (20 mM Tris-HCl, pH 7.0, 150 mM NaCl, 2 mM EDTA, 0.1% NP-40) and incubated for 1 h at 4 °C. Ni^{2+}-NTA resin or His^6-Prp19p 1-149 bound to Ni^{2+}-NTA resin were mixed with ^{35}S-labeled Cef1p-HA in binding buffer (20 mM NaPi, pH 7.0, 150 mM NaCl, 0.1% NP-40) and incubated for 1 h at 4 °C. MBP or MBP-Cwc2p 228–340 bound to amylose resin beads were mixed with ^{35}S-labeled Prp19p in binding buffer (20 mM Tris-HCl, pH 7.0, 150 mM NaCl, 2 mM EDTA, 0.1% NP-40) and incubated for 1 h at 4 °C. The beads were washed five times in binding buffer and the proteins were resolved by SDS-PAGE, treated with Amplify (Amersham Pharmacia Biotech), and exposed to film.

RNA and RT-PCR

Total RNA was prepared from cells by extraction with hot acidic phenol as described (Collart & Oliviero, 1993). First-strand synthesis was performed with the Superscript First-strand Synthesis System (Invitrogen) according to the manufacturer's directions. One hundred nanograms of RNA were used for each reaction. An oligonucleotide specific to the third exon of *DYN2* or the 3′ end of *CDC34* was used as the reverse primer for first-strand synthesis. After heat deactivation of the reverse transcriptase (RT) and subsequent RNase H treatment, one-tenth (2 μL) of each reaction was subjected to PCR using Taq polymerase (Qiagen) in a 50-μL reaction. 5′ primers were either DYN2F (Research Genetics) or 5′Cdc34. 3′ primers were either DYN2R (Research Genetics) or 3′Cdc34. Products were resolved on 0.8% agarose gel.

ACKNOWLEDGMENTS

We thank Liping Ren and Anna Feoktistova for valuable technical assistance, Jim Patton for providing useful suggestions, and Karim Labib for the degron reagents. This work was supported by National Institutes of Health Grant GM47728 (to K.L.G.). M.D.O. was supported by National Cancer Institute grant T32 CA09592. K.L.G. is an Associate Investigator of the Howard Hughes Medical Institute.

Received January 22, 2002; returned for revision February 13, 2002; revised manuscript received March 15, 2002

REFERENCES

Ajuh P, Kuster B, Panov K, Zomerdijk JC, Mann M, Lamond AI. 2000. Functional analysis of the human CDC5L complex and identification of its components by mass spectrometry. *EMBO J 19*:6569–6581.

Ajuh P, Sleeman J, Chusainow J, Lamond AI. 2001. A direct interaction between the carboxyl-terminal region of CDC5L and the WD40 domain of PLRG1 is essential for pre-mRNA splicing. *J Biol Chem 276*:42370–42381.

Aravind L, Koonin EV. 2000. The U box is a modified RING finger—A common domain in ubiquitination. *Curr Biol 10*:R132–134.

Ben-Yehuda S, Dix I, Russell CS, Levy S, Beggs JD, Kupiec M. 1998. Identification and functional analysis of hPRP17, the human homologue of the *PRP17/CDC40* yeast gene involved in splicing and cell cycle control. *RNA 4*:1304–1312.

Ben-Yehuda S, Dix I, Russell CS, McGarvey M, Beggs JD, Kupiec M. 2000a. Genetic and physical interactions between factors involved in both cell cycle progression and pre-mRNA splicing in *Saccharomyces cerevisiae. Genetics 156*:1503–1517.

Ben-Yehuda S, Russell CS, Dix I, Beggs JD, Kupiec M. 2000b. Extensive genetic interactions between *PRP8* and *PRP17/CDC40*, two yeast genes involved in pre-mRNA splicing and cell cycle progression. *Genetics 154*:61–71.

Bernstein HS, Coughlin SR. 1997. *Pombe* Cdc5-related protein. A putative human transcription factor implicated in mitogen-activated signaling. *J Biol Chem 272*:5833–5837.

Bernstein HS, Coughlin SR. 1998. A mammalian homolog of fission yeast Cdc5 regulates G2 progression and mitotic entry. *J Biol Chem 273*:4666–4671.

Berry LD, Feoktistova A, Wright MD, Gould KL. 1999. The *Schizosaccharomyces pombe dim1*(+) gene interacts with the anaphase-promoting complex or cyclosome (APC/C) component *lid1*(+) and is required for APC/C function. *Mol Cell Biol 19*:2535–2546.

Burns CG, Gould KL. 1999. Connections between pre-mRNA processing and regulation of the eukaryotic cell cycle. In: Chew SL, ed. *Post-transcriptional regulation of gene expression and its importance to the endocrine system.* Basel, Switzerland: Karger. pp 59–82.

Burns CG, Ohi R, Krainer AR, Gould KL. 1999. Evidence that Myb-related CDC5 proteins are required for pre-mRNA splicing. *Proc Natl Acad Sci USA 96*:13789–13794.

Burns CG, Ohi R, Mehta1 M, O'Toole ET, Clark TA, Sugnet CW, Ares M, Winey M, Gould KL. 2002. Removal of a single α-tubulin gene intron suppresses cell cycle arrest phenotypes of splicing factor mutations in *S. cerevisiae. Mol Cell Biol 22*:801–815.

Chen CH, Tsai WY, Chen HR, Wang CH, Cheng SC. 2001. Identification and characterization of two novel components of the Prp19p-associated complex, Ntc30p and Ntc20p. *J Biol Chem 276*:488–494.

Chen CH, Yu WC, Tsao TY, Wang LY, Chen HR, Lin JY, Tsai WY, Cheng SC. 2002. Functional and physical interactions between components of the Prp19p-associated complex. *Nucleic Acids Res 30*:1029–1037.

Chen HR, Jan SP, Tsao TY, Sheu YJ, Banroques J, Cheng SC. 1998. Snt309p, a component of the Prp19p-associated complex that interacts with Prp19p and associates with the spliceosome simultaneously with or immediately after dissociation of U4 in the same manner as Prp19p. *Mol Cell Biol 18*:2196–2204.

Chen HR, Tsao TY, Chen CH, Tsai WY, Her LS, Hsu MM, Cheng SC. 1999. Snt309p modulates interactions of Prp19p with its associated components to stabilize the Prp19p-associated complex essential for pre-mRNA splicing. *Proc Natl Acad Sci USA 96*:5406–5411.

Cheng SC, Tarn WY, Tsao TY, Abelson J. 1993. PRP19: A novel spliceosomal component. *Mol Cell Biol 13*:1876–1882.

Collart MA, Oliviero S. 1993. In: Ausubel FM, Brent R, Kinston RE, Moore DD, Seidman JG, Smith JA, Struhy K, eds. Basic protocol: Preparation of yeast RNA. *Current protocols in molecular biology*. New York: Wiley. pp 13.12.11–13.12.50.

Das R, Zhou Z, Reed R. 2000. Functional association of U2 snRNP with the ATP-independent spliceosomal complex E. *Mol Cell 5*:779–787.

Dash AB, Orrico FC, Ness SA. 1996. The EVES motif mediates both intermolecular and intramolecular regulation of c-Myb. *Genes & Dev 10*:1858–1869.

Dix I, Russell CS, O'Keefe RT, Newman AJ, Beggs JD. 1998. Protein–RNA interactions in the U5 snRNP of *Saccharomyces cerevisiae*. *RNA 4*:1675–1686.

Dohmen RJ, Wu P, Varshavsky A. 1994. Heat-inducible degron: A method for constructing temperature-sensitive mutants. *Science 263*:1273–1276.

Feng DF, Doolittle RF. 1996. Progressive alignment of amino acid sequences and construction of phylogenetic trees from them. *Methods Enzymol 266*:368–382.

Fikes JD, Becker DM, Winston F, Guarente L. 1990. Striking conservation of *TFIID* in *Schizosaccharomyces pombe* and *Saccharomyces cerevisiae*. *Nature 346*:291–294.

Frangioni JV, Neel BG. 1993. Solubilization and purification of enzymatically active glutathione S-transferase (pGEX) fusion proteins. *Anal Biochem 210*:179–187.

Freemont PS. 2000. RING for destruction? *Curr Biol 10*:R84–R87.

Gavin AC, Bosche M, Krause R, Grandi P, Marzioch M, Bauer A, Schultz J, Rick JM, Michon AM, Cruciat CM, et al. 2002. Functional organization of the yeast proteome by systematic analysis of protein complexes. *Nature 415*:141–147.

Gietz RD, Schiestl RH, Willems AR, Woods RA. 1995. Studies on the transformation of intact yeast cells by the LiAc/SS-DNA/PEG procedure. *Yeast 11*:355–360.

Gotzmann J, Gerner C, Meissner M, Holzmann K, Grimm R, Mikulits W, Sauermann G. 2000. hNMP 200: A novel human common nuclear matrix protein combining structural and regulatory functions. *Exp Cell Res 261*:166–179.

Gould KL, Moreno S, Owen DJ, Sazer S, Nurse P. 1991. Phosphorylation at Thr167 is required for *Schizosaccharomyces pombe* p34cdc2 function. *EMBO J 10*:3297–3309.

Groenen PM, Vanderlinden G, Devriendt K, Fryns JP, Van de Ven WJ. 1998. Rearrangement of the human CDC5L gene by a t(6;19)(p21;q13.1) in a patient with multicystic renal dysplasia. *Genomics 49*:218–229.

Guthrie C, Fink GR, eds. 1991. *Guide to yeast genetics and molecular biology.* San Diego, California: Academic Press, Inc.

Hatakeyama S, Yada M, Matsumoto M, Ishida N, Nakayama K. 2001. U-box proteins as a new family of ubiquitin-protein ligases. *J Biol Chem 276*:33111–33120.

Hirayama T, Shinozaki K. 1996. A *cdc5*+ homolog of a higher plant, *Arabidopsis thaliana*. *Proc Natl Acad Sci USA 93*:13371–13376.

Jackson PK, Eldridge AG, Freed E, Furstenthal L, Hsu JY, Kaiser BK, Reimann JD. 2000. The lore of the RINGs: Substrate recognition and catalysis by ubiquitin ligases. *Trends Cell Biol 10*: 429–439.

James P, Halladay J, Craig EA. 1996. Genomic libraries and a host strain designed for highly efficient two-hybrid selection in yeast. *Genetics 144*:1425–1436.

Jiang J, Ballinger CA, Wu Y, Dai Q, Cyr DM, Hohfeld J, Patterson C. 2001. CHIP is a U-box-dependent E3 ubiquitin ligase: Identification of Hsc70 as a target for ubiquitylation. *J Biol Chem 276*:42938–42944.

Koegl M, Hoppe T, Schlenker S, Ulrich HD, Mayer TU, Jentsch S. 1999. A novel ubiquitination factor, E4, is involved in multiubiquitin chain assembly. *Cell 96*:635–644.

Kramer A. 1996. The structure and function of proteins involved in mammalian pre-mRNA splicing. *Annu Rev Biochem 65*:367–409.

Labib K, Diffley JF, Kearsey SE. 1999. G1-phase and B-type cyclins exclude the DNA-replication factor Mcm4 from the nucleus. *Nat Cell Biol 1*:415–422.

Link AJ, Eng J, Schieltz DM, Carmack E, Mize GJ, Morris DR, Garvik BM, Yates JR III. 1999. Direct analysis of protein complexes using mass spectrometry. *Nat Biotechnol 17*:676–682.

Maroney PA, Romfo CM, Nilsen TW. 2000. Functional recognition of 5′ splice site by U4/U6.U5 tri-snRNP defines a novel ATP-dependent step in early spliceosome assembly. *Mol Cell 6*:317–328.

McDonald WH, Ohi R, Smelkova N, Frendewey D, Gould KL. 1999. Myb-related fission yeast cdc5p is a component of a 40S snRNP-containing complex and is essential for pre-mRNA splicing. *Mol Cell Biol 19*:5352–5362.

Murray HL, Jarrell KA. 1999. Flipping the switch to an active spliceosome. *Cell 96*:599–602.

Neubauer G, King A, Rappsilber J, Calvio C, Watson M, Ajuh P, Sleeman J, Lamond A, Mann M. 1998. Mass spectrometry and EST-database searching allows characterization of the multi-protein spliceosome complex. *Nat Genet 20*:46–50.

Ohi MD, Link AJ, Jennings JL, McDonald WH, Ren L, Gould KL. 2002. Proteomics analysis reveals stable multi-protein complexes in both fission and budding yeasts containing Myb-related Cdc5p/Cef1p, novel pre-mRNA splicing factors, and snRNAs. *Mol Cell Biol 22*:2011–2024.

Ohi R, Feoktistova A, McCann S, Valentine V, Look AT, Lipsick JS, Gould KL. 1998. Myb-related *Schizosaccharomyces pombe* cdc5p is structurally and functionally conserved in eukaryotes. *Mol Cell Biol 18*:4097–4108.

Pickart CM. 2001. Mechanisms underlying ubiquitination. *Ann Rev Biochem 70*:503–533.

Potashkin J, Kim D, Fons M, Humphrey T, Frendewey D. 1998. Cell-division-cycle defects associated with fission yeast pre-mRNA splicing mutants. *Curr Genet 34*:153–163.

Rigaut G, Shevchenko A, Rutz B, Wilm M, Mann M, Seraphin B. 1999. A generic protein purification method for protein complex characterization and proteome exploration. *Nat Biotechnol 17*:1030–1032.

Russell CS, Ben-Yehuda S, Dix I, Kupiec M, Beggs JD. 2000. Functional analyses of interacting factors involved in both pre-mRNA splicing and cell cycle progression in *Saccharomyces cerevisiae*. *RNA 6*:1565–1572.

Sakashita E, Sakamoto H. 1996. Protein-RNA and protein–protein interactions of the *Drosophila* sex-lethal mediated by its RNA-binding domains. *J Biochem* (Tokyo) *120*:1028–1033.

Samuels M, Deshpande G, Schedl P. 1998. Activities of the Sex-lethal protein in RNA binding and protein:protein interactions. *Nucleic Acids Res 26*:2625–2637.

Shamoo Y, Abdul-Manan N, Williams KR. 1995. Multiple RNA binding domains (RBDs) just don't add up. *Nucleic Acids Res 23*:725–728.

Smith TF, Gaitatzes C, Saxena K, Neer EJ. 1999. The WD repeat: A common architecture for diverse functions. *Trends Biochem Sci 24*:181–185.

Staley JP, Guthrie C. 1998. Mechanical devices of the spliceosome: Motors, clocks, springs, and things. *Cell 92*:315–326.

Stevens SW, Ryan DE, Ge HY, Moore RE, Young MK, Lee TD, Abelson J. 2002. Composition and functional characterization of the yeast spliceosomal penta-snRNP. *Mol Cell 9*:31–44.

Stukenberg PT, Lustig KD, McGarry TJ, King RW, Kuang J, Kirschner MW. 1997. Systematic identification of mitotic phosphoproteins. *Curr Biol 7*:338–348.

Tarn WY, Hsu CH, Huang KT, Chen HR, Kao HY, Lee KR, Cheng SC. 1994. Functional association of essential splicing factor(s) with PRP19 in a protein complex. *EMBO J 13*:2421–2431.

Tarn WY, Lee KR, Cheng SC. 1993a. Yeast precursor mRNA processing protein PRP19 associates with the spliceosome concomitant with or just after dissociation of U4 small nuclear RNA. *Proc Natl Acad Sci USA 90*:10821–10825.

Tarn WY, Lee KR, Cheng SC. 1993b. The yeast PRP19 protein is not tightly associated with small nuclear RNAs, but appears to associate with the spliceosome after binding of U2 to the pre-mRNA and prior to formation of the functional spliceosome. *Mol Cell Biol 13*:1883–1891.

Tasto JJ, Carnahan RH, McDonald WH, Gould KL. 2001. Vectors and gene targeting modules for tandem affinity purification in *Schizosaccharomyces pombe*. *Yeast 18*:657–662.

Thompson JD, Higgins DG, Gibson TJ. 1994. CLUSTAL W: Improving the sensitivity of progressive multiple sequence alignment through sequence weighting, position-specific gap penalties and weight matrix choice. *Nucleic Acids Res 22*:4673–4680.

Tsai WY, Chow YT, Chen HR, Huang KT, Hong RI, Jan SP, Kuo NY, Tsao TY, Chen CH, Cheng SC. 1999. Cef1p is a component of the Prp19p-associated complex and essential for pre-mRNA splicing. *J Biol Chem 274*:9455–9462.

Tyers M, Jorgensen P. 2000. Proteolysis and the cell cycle: With this RING I do thee destroy. *Curr Opin Genet Dev 10*:54–64.

Verhasselt P, Volckaert G. 1997. Sequence analysis of a 37.6 kbp cosmid clone from the right arm of *Saccharomyces cerevisiae* chromosome XII, carrying *YAP3*, *HOG1*, *SNR6*, tRNA-Arg3 and 23 new open reading frames, among which several homologies to proteins involved in cell division control and to mammalian growth factors and other animal proteins are found. *Yeast 13*:241–250.

Zhang K, Smouse D, Perrimon N. 1991. The *crooked neck* gene of *Drosophila* contains a motif found in a family of yeast cell cycle genes. *Genes & Dev 5*:1080–1091.